SAPIENZA
Università di Roma
Facoltà di Farmacia e Medicina

Ph.D. in
MORPHOGENESIS AND TISSUE ENGINEERING

XXXV Ciclo
(A.A. 2021/2022)

Role of m^{6}A-dependent circRNAs during stress response in myeloid leukemic cells

Ph.D. Student
Alessia Iaiza

Tutors
Prof. Francesco Fazi
Dr. Silvia Masciarelli

Coordinator
Prof. Antonio Musarò

CONFIDENTIALITY NOTICE

Reviewers and PhD committee members are obliged to keep the files confidential and to delete all records after completing the review process.

Receipt of scientific papers, in order to obtain the title of PhD, as a committee member of PhD course in Morphogenesis and Tissue Engineering requires compliance with the following regulations:

I. consider the Confidential and Reserved Information as strictly private and take all reasonable steps to keep it that way.
II. use the confidential and reserved information only for the purpose for which it was provided or disclosed, undertaking not to disclose the information contained in the documents received to third parties.
III. to guarantee maximum confidentiality, also in compliance with the current legislation on trademarks, copyrights and patents for industrial inventions and on the basis of the privacy legislation, pursuant to Legislative Decree 196/2003, regarding know-how and all the information acquired, which cannot in any way, in any case and for any reason be used for one's own or others' profit and / or be disclosed and/or reproduced or otherwise disclosed to third parties.

INDEX

1. SUMMARY

The biological issue. N6-methyladenosine (m^6A) is one of the most prevalent, abundant and conserved RNA modifications. It controls several biological processes, including also the biogenesis and function of circular RNAs (circRNAs), which are a class of covalently closed single-stranded RNAs. Recently, it has emerged a molecular interaction between the m^6A RNA modification factors and the suppression of the proteotoxic stress response which induction is emerging as a relevant anticancer therapy in Acute Myeloid Leukemia (AML).
Since proteasome inhibition, leading to imbalance in protein homeostasis, is strictly linked to the stress response induction, we decided to investigate the effect of Bortezomib (Btz) on m^6A enzymes expression and its impact on the modulation of m^6A-dependent circRNAs expression.
Results. In this thesis, we show that treatment of AML cells with Btz induces m^6A enzymes downregulation at translation level. Moreover, we evidenced that this modulation is mediated by ROS generation and activation of the oxidative stress response. Indeed, administration of the reducing agent N-acetylcysteine inhibits Btz-mediated m^6A enzymes downregulation. Moreover, despite the general decrease of m^6A modification levels, we found that some circRNAs are more methylated and expressed upon Btz treatment compared to control samples.
Conclusion. All together these data allow us to identify and investigate specific m^6A-dependent circRNAs involved in the response to proteotoxic stress generated by Btz, in order to exploit them as molecular targets to improve Btz effectiveness in AML.

2. INTRODUCTION

2.1 N6-methyladenosine (m^6A)

Among more than 150 types of post-transcriptional RNA modifications, N6-methyladenosine (m^6A) is one of the most prevalent modifications in eukaryotic mRNAs. It was discovered in 1974[1] and the enzyme responsible of this modification was purified in the 1990s from HeLa nuclear extract (MTA complex)[2], but only in the last decades, thanks to the technological advances, it has been possible to know more about it. Indeed, in 2012 Dominissini at al. introduced m^6A-seq, a valuable tool that allows to map this modification with an anti-m^6A antibody, and identified the consensus motif RRm^6ACH ([G/A/U][G>A]m^6AC[U>A>C]) in the transcript of more than 7000 human genes. In particular, m^6A modification occurs around the stop codon at 3'UTR and within long internal exons[3,4,5]. Like DNA methylation, m^6A modification is dynamic and reversible, regulated by methyltransferase enzymes, also known as writer enzymes, and demethylase enzymes, or eraser enzymes.

M^6A methyltransferase complex consist of a dimer, called MAC, formed by METTL3 and METTL14 and it is localized in the nucleus, particularly at the level of the nuclear speckles. The crystallographic structure revealed that METTL3 is the catalytic subunit of this complex, which has the ability to bind SAM (S-adenosylmethionine), the methyl group donor for all methyltransferases, while METTL14 acts as an RNA binding platform[6]. MAC complex alone is able to methylate the RNA *in vitro*, but not *in vivo*, where it is associated with a regulatory complex, named MACOM. MACOM complex is composed by:

- RBM15, which recruits m^6A methyltransferase complex to pre-mRNA target site[7];
- WTAP (Wilms' tumor 1-associating protein), which directly interacts with METTL3 and mediates the tethering of m^6A complex to RNA and the nuclear speckles localization of METTL3-METTL14 dimer. It is a ubiquitously expressed protein, without any

catalytic domain, nonetheless its knockdown resulted in a 6.25-fold decrease in m^6A levels, so it has important regulatory functions [7,8].
- KIAA1429, also known as VIRMA (vir-like m^6A methyltransferase associated), recruits the complex on the mRNA target; in particular it is responsible for m^6A deposition at the 3′UTR and correlates with alternative polyadenylation[9].
- ZC3H13, a zinc finger protein recently discovered, is required for RBM15 and WTAP association. It modulates m^6A RNA modification in the nucleus, indeed its knockout induces a decrease of 80% in m^6A levels[10,11].
Other methyltransferase enzymes are METTL16, METTL5 and ZCCHC4. METTL16 differs significantly from METTL3/METTL14 in the primary sequence (with less than 13% identity to the catalytic domain of METTL3), stoichiometry (it works as a monomer and not as a dimer) and the RNA methylation consensus sequence (UACAGARAA)[12]. Originally it was expected to mediate m^6A methylation of rRNA, but to date MAT2A, an S-adenosylmethionine synthase, and U6 small nuclear RNA (snRNA) have been identified as METTL16 targets[13]. Notably, METTL16 regulates both splicing and stability of MAT2A mRNA, by directly binding the hairpin structures in the 3'UTR, in response to intracellular SAM changes[13,12]. ZCCHC4 and METTL5 are responsible for 28S and 18S rRNA m^6A modification, respectively[14,15].
Removal of m^6A is mediated by the FTO and ALKBH5 demethylases, both belonging to the ALKB subfamily of the superfamily of Fe(II)/2-oxoglutarate dioxygenases[16,17]. FTO has been associated with human body weight, while ALKBH5 with mouse fertility[18].
In 2011, Guifang Jia at al., showed that FTO (fat mass and obesity-associated protein) localizes in the nuclear speckles and is able to demethylate m^6A in vitro. Indeed its depletion leads to increased m^6A modification levels[16]. However, recent work has shown that the main target of FTO demethylase is the N62′-O-dimethyladenosine (m^6Am) modification, with a 100-fold higher catalytic activity than

for N6-methyladenosine[19], for this reason its role in the demethylation of m^6A is still debated.
The second identified m^6A demethylase is ALKBH5, which, unlike other ALK family members that can catalyze the demethylation of double-stranded substrates, revealed demethylation activity with a preference for single-stranded RNA/DNA[20]. In particular, ALKBH5 modulates mRNA export and its overexpression in HeLa cells leads a 29% of m^6A levels reduction, while its knockout in male mice showed a reduced fertility due to aberrant spermatogenesis and apoptosis in the testis[17,7].
There are numerous reader proteins, each capable of influencing different RNA metabolism steps. M^6A reading can take place in two different ways, direct and indirect. In the latter one, the addition of the methyl group on adenosine induces a structural change in RNA caused by m^6A-U pair energetically unfavorable, modulating the binding of reader proteins[21]. This mechanism, that regulates RNA-protein interactions in an m^6A-dependent manner and remodels RNA structure, is called 'm^6A-switch'. The m^6A reader heterogeneous nuclear ribonucleoprotein C (HNRNPC) is an abundant nuclear RNA-binding protein, which influences RNA stability, splicing, export and translation[22,23,24]. It has been demonstrated that m^6A-mediated RNA destabilization induces a single-stranded HNRNPC binding motif exposure facilitating HNRNPC protein binding[25,26]. Different following works have shown that other ribonucleoproteins are also able to bind m^6A. For example, HNRNPA2B1 protein is an m^6A reader that regulates alternative splicing and nuclear processing of a subset of microRNAs[27]. Moreover, Zhou K. et al., demonstrated how the presence of m^6A modification can promote hnRNPG binding to modulate RNAPII occupancy and alternative splicing[28].
The other way is the direct one with the recruitment of specific proteins or protein complexes. Certainly, a primary role is played by proteins belonging to the YT521-B homology (YTH) domain-containing protein family[29]. Five members of this family have been identified, with an aromatic cage that preferentially recognizes and

bind the GG(m^6A)C sequence, classified into three categories: YTHDC1 (YTH domain-containing protein 1), YTHDC2 (YTH domain-containing protein 2), and YTHDF (YTH domain-containing family protein) family, formed by YTHDF1, YTHDF2, YTHDF3[30,31,32].

YTHDC1 is a nuclear reader protein that regulates alternative splicing and polyadenylation, as it directly binds the m^6A-bearing exon, attracts and, more efficiently, binds the SRSF3 protein, promoting exonic inclusion[33]. A further role of YTHDC1 is to indirectly increase translation, since its binding to SRSF3 allows binding to NXF1 or TAP (nuclear RNA export factor) and promotes nuclear export[34].

YTHDC2 is a cytosolic reader, with the YTH domain capable of recognizing the m^6A modification, but with a lower affinity than the other family members[35]. In addition, YTHDC2 possesses a domain with 3'→5' helicase activity, in particular it is able to recognize U-rich motifs at the 3'UTR and to bind RNA independently of the presence of m^6A modification. YTHDF2 depletion results in mice infertility; in fact it is mainly expressed in the animal germ line, where it interacts with MEIOC and 5'→3' exoribonuclease XRN1[36,37].

YTHDF1/2/3 also are cytosolic readers and all of them have an important role in mRNA stability. YTHDF1 depletion leads to a drastic decrease in the translation efficiency of m^6A modified mRNAs and this decrease is positively correlated with the number of m^6A-bearing sites and the percentage of silencing. Indeed, it has been demonstrated that YTHDF1 enhances translation in an m^6A-dependent manner by interacting directly with translation initiation factors, like eIF3, and ribosomes[18]. YTHDF2 plays an important role in female fertility, as it induces maternal RNA degradation, allowing oocyte maturation[38]. In particular, C-YTHDF2 selectively recognizes and binds m^6A modification, while N-YTHDF2 binds the CCR4-NOT deadenylation complex and localizes the YTHDF2-m^6A-mRNA complex in P-bodies[39,40].

YTHDF3 shares half of its targets with YTHDF1 and the other half with YTHDF2. In fact, it promotes the translation of messengers in synergy with YTHDF1 e influences RNA degradation mediated by YTHDF2[41].

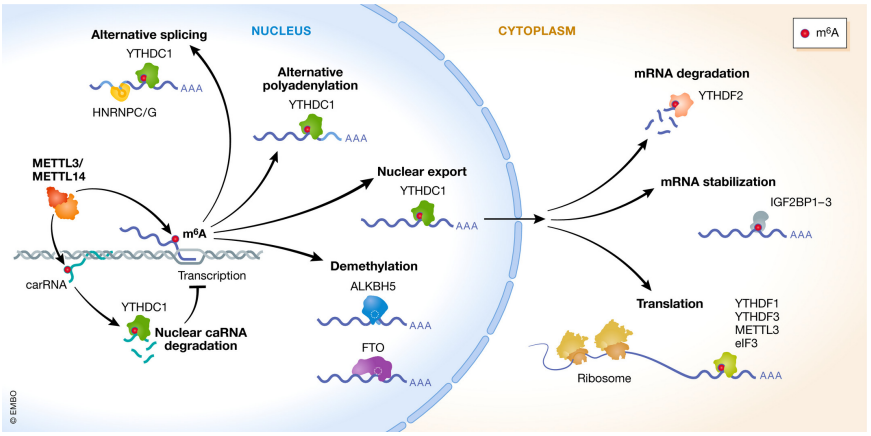

Figure 2.1. Machineries responsible for m^{6}A deposition, reading and removal. The methyl group on the N6 of adenosine is added by the methyltransferase complex formed by METTL3, METTL14, WTAP, KIAA1429; m^{6}A modification is read by a family of YTH proteins, but also by the HNRNP ribonucleoproteins and it is removed by the ALKBH5 and FTO erasers.

2.2 Function of N6-methyladenosine

As we have seen so far, m^{6}A modulates all RNA metabolism steps, leading to the regulation of various cellular processes, both physiological and non-physiological. As previously described, m^{6}A modification plays a key role in the reproductive system development and in the proper formation of the embryo. Moreover, m^{6}A has an important role in the maintenance of the circadian rhythm and the cell cycle, both of which are regulated by the transient and sequential activation of genes and cyclins, respectively[42,43]. N6-methyladenosine finely tunes cell differentiation, for example, during pre-adipocyte differentiation

FTO was uncovered to regulate exonic splicing of RUNX1T1 by regulating m^6A modifications around splice sites[44].
Several studies highlighted the role of m^6A in development of the hematopoietic system and maintenance of pluripotency of hematopoietic stem cells. Zhang C. at al. have demonstrated the critical role of m^6A in determining HSPCs cell fate during the endothelial-to-hematopoietic transition (EHT) [45]; furthermore the methyltransferase complex is required for differentiation and quiescence of adult HSCs[46,47].

2.3 circRNAs

circular RNAs are a class of covalently closed single stranded RNAs identified in plant viroids more than 40 years ago and subsequently also in the cytoplasm of eukaryotic cells[48,49]. In the following years, different research groups identified these stable, conserved and circular molecules without 5' N7-methylguanosine (m^7G) caps and 3'polyadenylated tails, in which exons were joined at the consensus splice site, but with an inverted order[50,51]. In the last 10 years, the recent advances in RNA sequencing (RNA-seq) with bioinformatics tools for circular RNA annotation, have highlighted the extensive expression of circRNAs in tissue- and cell type-specific manner[52,53,54,55,56]. In the majority of cases, circRNA are generated by a different kind of splicing, named back-splicing, in which the 3' end of an exon binds the 5' end of an upstream exon, forming a circular structure, with a back-splicing junction site (BSJ). Alternatively, intron lariats, during exon skipping, can escape debranching and form an intronic circRNA with a 2′,5′-phosphodiester bond[57,58].
Although circRNAs biogenesis competes with pre-mRNA splicing, because is dependent on the canonical splicing machinery, there are different mechanisms which favor the biogenesis of circRNAs[59].
Back-splicing can be promoted/mediated by base pairing between Alu elements[60], localized in upstream and downstream introns, but also by RNA-binding proteins (RBPs) dimerization, such as FUS

and QKI[61,62]. The alternative splicing factor, Quaking (QKI) binds pre-mRNA at both intronic regions bordering the circularized exons and dimerizes by facilitating the formation of an RNA loop and back splicing[63]. Similarly, the muscleblind splicing factor regulates circMbl biogenesis and vice versa. In particular, Yuan Y. et al. demonstrated that circMbl flanking intronic regions have different binding sites for MBL, which are bound by the latter to promote circMbl production and regulate MBL levels[64].
Recently it has been reported that also the presence of m^6A RNA modification can favor back-splicing and therefore circRNAs formation[65].
The efficiency of back splicing is lower compared to that of canonical splicing, hence the general amount of circRNAs is low in cells and tissues. Nevertheless, they remain stable with half-lives ranging from 18.8 to 23.7 h (compared with 4.0–7.4 h for their cognate linear RNAs), because they are resistant to the linear RNA decay machinery[66].

2.4 Function of circRNAs

According to the presence or not of introns, circRNAs can be localized in the nucleus or can be exported in the cytoplasm by RNA helicase DDX39B/39A in a length-dependent manner (DDX39B is required for export of long circRNAs, while DDX39A for export of short circRNAs)[67].
Extron-Intron circRNAs (EIciRNAs), localized in the nucleus, can interact with U1 snRNP and RNA Pol II, enhancing or reducing the transcription of their parental gene[59,68]. Some EIciRNAs hybridize to host locus DNA forming RNA:DNA hybrids (R-loops) and therefore they can regulate transcription in different ways: stalling the RNA Pol II, promoting exon skipping and therefore regulating the alternative splicing , recruiting transcription factors (TFs)[69].
The most common function is certainly to act as microRNA (miRNA) sponge. One circRNA can have multiple binding sites for the same miRNAs or different binding sites for different miRNAs.

The first circRNA identified as miRNA sponge was Cerebellar degeneration-related protein 1 antisense RNA (CDR1as), also known as circular RNA sponge for miR-7 (ciRS-7). ciRS-7 harbours approximately 63 binding sites for miR-7 and by sponging miR-7 in neuronal tissues it plays a crucial role in midbrain development[70]. Furthermore, CDR1 regulates several physiological and pathological aspects since it act as miRNA sponge for a variety of different miRNAs[71].

circRNAs can also modulate mRNA stability. For example, circCDR1as forms a duplex structure with CDR1 mRNA and inhibits its cleavage mediated by Ago2, while circRasGEF1B positively regulates the stability of mature ICAM-1 mRNAs[72,73].

Another important function of circRNAs is to bind RNA binding proteins (RBPs). CircRNAs can bind RBPs to regulate them, acting like protein sponge, decoy, scaffold or recruitment platforms. An example of function of a circRNA as protein scaffold is circ-Fox3, highly expressed in non-neoplastic cells, where it negatively regulates the cell cycle. Usually, the cell cycle protein cyclin-dependent kinase 2 (also known as cell division protein kinase 2 or CDK2) binds cyclin A and E and allows cell cycle progression while cyclin-dependent kinase inhibitor 1 (or p21) prevents this binding by arresting the cell cycle. Circ-Fox3 binds both CDK2 and p21 forming circ-Foxo3-p21-CDK2 ternary complex; p21, being close to CDK2, inhibits CDK2 blocking cell cycle[74].

For a long time, circRNAs were considered non-coding RNAs, due to the lack of the polyA tail at 3' and 7-methylguanosine cap at 5', which are necessary for the initiation of translation. However, several studies have demonstrated that circRNAs can be translated into peptides in a cap-independent manner due to the presence of internal ribosomal entry sites (IRES)[75].

Recently, it has been shown that some circRNAs, lacking IRES, can be translated into peptides due to the presence of the m^6A modification, read by YTHDF2, which binds the translation initiation factor eIF3[76].

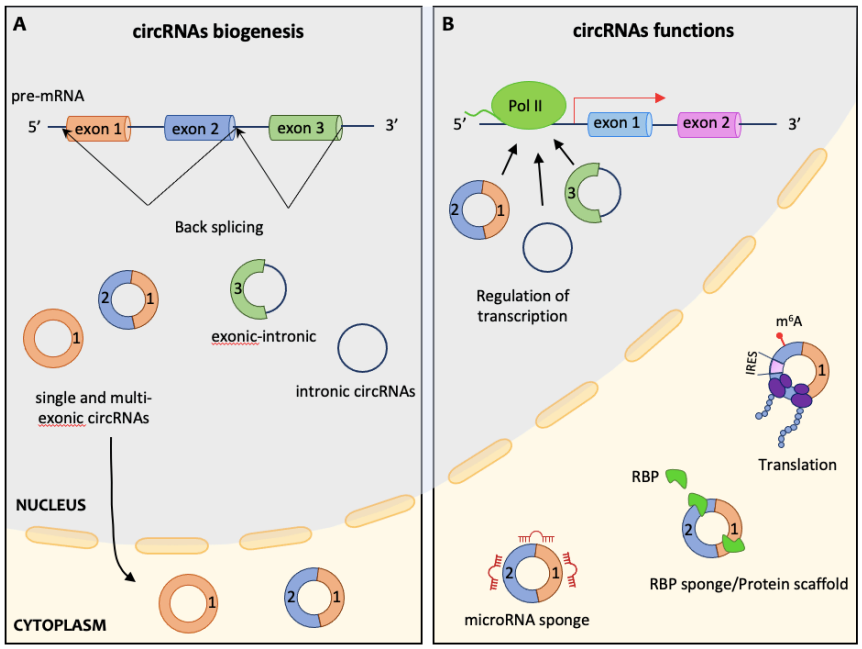

Figure 2.2. circRNAs biogenesis and function. circRNAs are generated by back-splicing, in which the 3' end of an exon binds the 5' end of an upstream exon. Based on the presence or not of introns they can be classified into three main classes: single or multi-exonic circRNAs (on the left); exonic-intronic circRNAs (in the middle) and intronic-circRNAs (on the right). In the nucleus circRNAs regulate mainly the transcription, interacting with the Polymerase-II. In the cytoplasm they act as miRNA sponges, as RBP sponges/scaffold and they can be also translated thanks to the presence of an IRES or m^6A modification[77].

Due to their tissue- and cell-specific expression and stability in body fluids, such as saliva, blood, urine, and especially plasma, circRNAs may be considered a promising biomarker for cancer diagnosis. The expression of certain circRNAs may be different among various types of tumors, as well as in different subtypes of the same disease. Not only that, their expression changes during disease progression, depending on stage and clinical outcome. Numerous studies have shown an enrichment of circRNAs in exosomes, where they are

protected from the surrounding environment and can be targeted to specific target cells, allowing intercellular communication even over long distances[78].

2.5 AML

Among the enormous heterogeneity of blood diseases, the most common is certainly acute myeloid leukemia, with an annual overall incidence of 3.8 cases per 100,000 in the US and Europe[79]. AML is characterized by the uncontrolled accumulation of uncompletely differentiated myeloid cells, especially granulocytes or monocytes that are part of innate immunity and thus important in responding to any pathogen in the first line. This is the reason why this disease is so inauspicious, with the 5-year overall survival (OS) of less than 5% in patients older than 65 years[80]. Although it mainly affects the elderly, it can occur also in adults and children[81].
The most common symptoms are general tiredness, high temperature or feeling feverish and frequent short or long time infections, easily bruising and bleeding and weight loss.
Because of the heterogeneity of this disease, a classification criterion became indispensable. The French–American–British classification system or FAB, dated back to 1976, was the first system used to classify AML and it divides AML into 8 histotypes (M0-M7) based on the morphological and cyto-chemical characteristics of the leukemic cells[82].
In 2001, the World Health Organization (WHO) introduced a new classification criterion that has undergone subsequent revisions and takes into account new clinical, prognostic, morphological, immunophenotypic and genetic data collected so far[83,84,85].
From the 2016 revision, it is possible to identify 6 subtypes of AML which in turn are subdivided into multiple subtypes: AML with recurrent genetic abnormalities; AML with myelodysplasia-related features; therapy-related AML; AML not otherwise specified; myeloid sarcoma and Down syndrome-related myeloid proliferation[84].

One of the most common genetic abnormalities is the Internal Tandem Duplication of FLT3 gene, also known as FLT3-ITD. FLT-3 is a receptor tyrosin kinase that regulates hematopoietic cell differentiation. The duplication occurs in the self-inhibitory domain of the receptor causing constitutive activation and hindrance of regulation of the receptor[86]. Furthermore, the FLT3-ITD mutation and its improper processing in the ER, causes its retention in this organelle and an increase in reactive oxygen species (ROS), resulting in DNA double-strand breaks (DSB) and repair errors that may explain the aggressiveness of AML in FLT3/ITD patients[87,86].
Among the chromosomal translocations, it is certainly worth mentioning the PML-RARA translocation, a prognostic factor of acute promyelocytic leukemia (APL), and the MLL-fusion protein (Mixed Lineage Leukemia fusion protein)[88]. To date, more than 60 translocation partner genes (TPGs) have been characterized, but the most common are MLL-AF4, MLL-AF9, MLL-ENL and MLL-AF10[89].
For a long time, the standard treatment for AML was the '3 + 7 regimen' (3 days daunorubicin + 7 days cytarabine) in younger patients, (usual upper age limit 60-65 years), as older patients do not tolerate this intense chemotherapy regimen. Through the study of genetic and molecular characteristics, it has been possible to design targeted therapies. For example, the use of chemotherapy-free regimens consisting of the combination of trans-retinoic acid (ATRA) and arsenic trioxide in APL have led to cure rates of 90%[90].
Although the 3+7 regimen is still the treatment of choice in most cases, the development of new strategies and drug combinations allowed the set up of a variety of clinical trials, with promising results. Indeed, there are targeted therapies, such as the use of FLT3 inhibitors (gilteritinib, sorfenib, midostaurin) in FLT3-mutated AML or of monoclonal antibodies (GO, novel CD33 monoclonal antibodies)[91]. Antigen chimeric receptor (CAR)-T cell trials are ongoing, including autologous and allogeneic CART cells (targeting CD123, CD33 and CLL1)[92].

2.6 m^{6}A and AML

As described above, AML is a highly heterogeneous blood malignancy with a high mortality rate and current therapies need to be continuously updated to increase survival rates. In recent years, there has been increasing interest in m^{6}A and its role in cancer and hematological diseases. WTAP was one of the first m^{6}A regulatory factors to be discovered, when this modification was not yet known, as a specific interactor of the Wilms' tumor gene (WT1), a transcription factor very important for cell survival and development[93]. Initially, WT1 was identified as a tumor suppressor, as it is able to inhibit cell growth, but in recent years, its role as an oncogene has also been highlighted, especially in leukaemias[94]. Following the discovery of the interaction between WTAP and WT1, attention shifted to WTAP study. Several works highlighted overexpression of this factor in AML patients, where WTAP has an oncogenic role, as it has pro-survival and pro-proliferative activity by regulating the methylation of c-MYC mRNA and rendering AML cells resistant to chemotherapy drugs[95,96].
In the following years, different research groups have investigated the role of the MACOM methyltransferase complex. METTL3 and METTL14 have been found to be over-expressed in hematopoietic stem cells (HSCs), where they play an important role in maintaining stemness by regulating proliferation. During normal hematopoiesis, the expression of METTL3 and METTL14 decrease to allow differentiation of HSCs into myeloid precursors and then myeloid cells. However, it has been shown that in AML, the expression of these enzymes remains consistently high, leading to uncontrolled proliferation of leukemic stem cells (LSCs)[97,98].
Vu at al., demonstrated how METTL3 overexpression in AML is important for methylating and increasing the translation efficiency of PTEN, BCL2 and c-MYC mRNAs[99]. Furthermore, METTL3 is recruited by the transcription factor CEBPZ (CCAAT enhancer binding protein) to the transcription start sites of genes important in hematopoietic differentiation[97]. In AML, METTL3 has been

observed mis localized in the cytoplasm where it associates with translating ribosomes and regulates targeted mRNA translation, among which WTAP, independent of its catalytic activity[100].
Also METTL14 plays a pro-tumoral role in AML. METTL14 is highly expressed in HSCs and is negatively regulated by SPI1, a transcriptional master regulator of myeloid cells, which is poorly expressed in HSCs. In normal differentiation, SPI1 levels increase, allowing inhibition of METTL14 and differentiation of myeloid precursors. In AML, SPI1 expression is suppressed, resulting in high expression of METTL14, which positively regulates MYC and MYB expression, leading to enhanced self-renewal/proliferation of LSCs and block myeloid differentiation[98].
According to genome-wide gene expression profiling datasets, FTO is highly expressed in AMLs carrying t(11q23)/MLL-rearrangements, t(15;17)/PML-RARA, FLT3-ITD, and/or NPM1 mutations. FTO overexpression induces leukemic cells proliferation and transformation and inhibits apoptosis, enhancing leukemogenesis. Interestingly, FTO demethylates and destabilizes ASB2 and RARA mRNAs, key regulators in normal hematopoietic differentiation and in ATRA-induced differentiation of leukemia cell[101].
Shen at al., have reported that also ALKBH5 is abnormally expressed and correlates with a poor prognosis in AML. In particular, they demonstrated that ALKBH5 is required for AML cell proliferation and transformation, as well as for LSCs self-renewal, but it is not essential for normal hematopoiesis[102].
Recently, it has been shown that in AML, ALKBH5 locus shows increased chromatin accessibility due to high expression levels of the histone demethylase KDM4C, promoting TFs recruitment, among which MYB, and Pol II-CTD to the ALKBH5 promoter. The resulting increased expression of ALKBH5 leads to the stabilization of AXL transcript involved in PI3K, MAPK, JAK/STAT, and NF-κB signaling, associated with AML chemoresistance[103].
Regarding m^6A readers, YTHDF2, YTHDC1 and IGF2BP1 have been found overexpressed in AML so far. All of them are required

for the development and maintenance of LSCs: YTHDF2 induces degradation of the tumor necrosis factor receptor Tnfrsf2, which is involved in cell death, YTDC1 regulates MCM4, which is a critical regulator of DNA replication, while IGF2BP1 controls the critical self-renewal regulators HOXB4 and MYB, and the aldehyde dehydrogenase expression, ALDH1A. YTHDC1 is essential for normal hematopoiesis, as opposed to YTHDF2[104,105,106].

2.7 circRNAs and AML

A genome-wide study of 6 bone marrow samples from pediatric AML patients, found more than 550 differentially expressed circRNAs. Half of these circRNAs promote leukemic cell growth and restrained apoptosis by sponging different tumor suppressor miRNAs, while the others act in the oppositive way. An example of the last, is circ_0001947, which expression levels negatively correlate with BM or PB percentage in AML patients. Both *in vitro* and *in vivo* studies have indeed shown that circ_0001947 is able to inhibit both proliferation and apoptosis in AML, acting as a sponge of the hsa-miR-329-5p restoring the expression of the hsa-miR-329-5p target gene CREBRF, a potent tumor suppressor[107].
A very interesting case is circMYBL2, which is highly expressed in FLT3-ITD positive AML, which accounts for 25% of all AML. CircMYBL2 is derived from the circularization of the MYB2 gene locus, which is involved in cell cycle control. Sun et al., demonstrated that circMYBL2, through recruitment of the RBP PTBP1, enhances the binding of the latter to FLT3 mRNA by increasing its translation efficiency and consequently activating of FLT3-ITD-dependent protumor signaling pathways[108].
As seen above and as it is well known, several AML subtypes exhibit translocations and inversions leading to the formation of fusion proteins, including PML-RARA, MLL-AF9, MLL-AF4. Several fusion circRNAs (f-circRNAs) have been identified, among which f-circM9 and circAF4. F-circM9 is the product of MLL-AF9 fusion transcript circularization, highly expressed in AML, where it

has an oncogenic role inducing leukemia progression *in vivo*. Furthermore, f-circM9 is able to bestow a survival advantage to tumor cells in response to therapy treatment with Arsenic trioxide (ATO) and cytarabine (Ara-C)[109]. Regarding circAF4, there are actually four isoforms of this circRNA originating from the MLL-AF4 fusion partner gene. One of these four circRNA isoforms is highly expressed in AML, named with the generic name of circAF4; it sequesters miR-128-3p allowing the expression of MLL-AF4[110]. Multiple mechanisms lead to drug and chemotherapy resistance of LSCs, including those mediated by the ATP-binding cassette (ABC) transporter-mediated multidrug resistance proteins, mutated FLT3 and others. In recent years, it emerged that circRNAs can also confer drug resistance, but the molecular mechanisms are still unclear. The study by Shang J. et al. showed that circPAN3 is able to confer doxorubicin (ADM) resistance, as it is differentially expressed between drug-resistant THP-1/ADM cells and naive THP-1 cells. CircPAN3, acting as a sponge for miR-153-5p and miR-183-5p, enables the activation of XIAP, belonging to the inhibitor-of-apoptosis proteins (IAPs), endogenous caspase inhibitors[111].

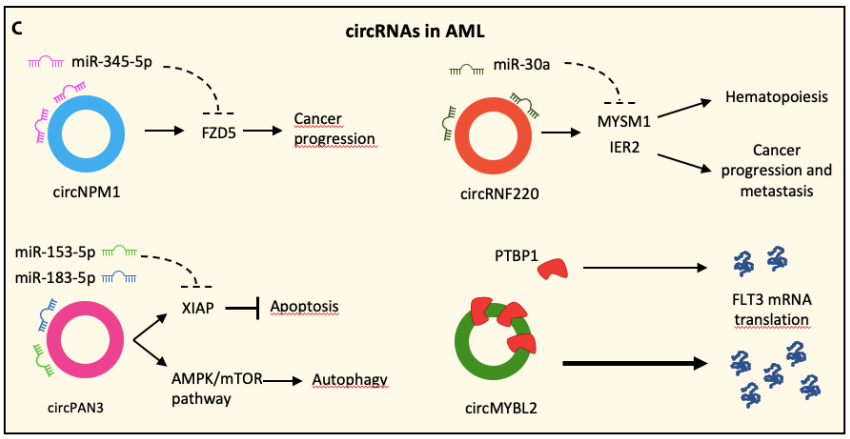

Figure 2.3. Molecular mechanisms of circRNAs involved in AML. In this figure, it has been reported some of the circRNAs involved in leukemia. circNPM1 and circRNF220 target miR-345-5p and miR-30a, respectively, and promote cancer progression. On the other hand, circPAN3 is involved in drug resistance mechanisms by inhibiting cell death and circMYBL2, highly expressed

in FLT3-ITD positive AML, enhances AML progression through PTBP1 binding and consequent increase in FLT3 mRNA translation efficiency.

2.8 m^{6}A modification and circRNAs network involvement in proteostasis

The network of cellular mechanisms that regulate protein synthesis, maturation and degradation is called proteostasis and its balance is essential for cell homeostasis. Among these mechanisms there are the Unfolded Protein Response (UPR), the endoplasmic reticulum (ER)-associated degradation (ERAD) and autophagy which are key processes for proper cellular and organism development and maintenance. Alterations in any of these processes can lead to development of various diseases as well as tumorigenesis. Some types of cancer have used these processes to their advantage to overcome the physiological check points of the cell, but also to escape the treatments in use today. There is a wide range of stresses that can disrupt protein homeostasis and activate what is called the integrated stress response (ISR)[112]. Among the extrinsic cellular stimuli there are hypoxia, amino acid deprivation, glucose deprivation, and viral infection, while as far as intrinsic stimuli are concerned, the endoplasmic reticulum (ER) stress rather than oxidative stress, or in the case of tumors, the activation of certain oncogenes play an important role[113,114].
All these stimuli lead to phosphorylation and de-activation of the translation initiation factor eIF2α, resulting in a decrease of general protein synthesis to reduce proteostatic stress and to allow the cell to increase its capacity to deal with proteostasis alteration by translation of specific mRNAs, including that of the activating transcription factor 4 (ATF4) [115]. In case of a very strong or long-lasting stress, the ISR will not be able to overcome the adaptive stress response and cell death pathways will be activated[116,113].
Neoplastic cells must to adapt to the stresses induced by DNA damage, lack of metabolites, oxidation, but also by chemotherapeutic drugs, in order to survive. In recent years,

research has heavily focused on understanding the molecular mechanisms of the fine-tuned stress responses governing cell survival/death, with the aim of exploiting them as possible therapeutic targets. In AML, enormous progresses have been made in this field. In particular, since AML is often characterized by mutant and fusion proteins that are more prone to misfolding, it is a good model of tumor cell that could be more susceptible to pharmacological alteration of proteostasis, in terms of ER stress and oxidative stress for example, relatively to healthy cells.

There is a significant cross-talk between ER stress and oxidative stress. Unbalance in ER homeostasis causes accumulation of misfolded proteins in the lumen, defined ER stress. In this case, the three ER stress sensors IRE1, PERK and AT6 are activated, triggering the UPR, and in turn activate the transcription factors XBP1, ATF4 and AT6 to promote expression of genes required to resolve the stress (chaperones, ERAD proteins, etc)[117].

Under ER stress conditions, the failure to achieve proper protein folding causes increased disulphide bond shuffling, which leads to accumulation of reactive oxygen species (ROS), resulting in the release of Ca^{2+} into the cytoplasm and in the production of further ROS(ref). ROS, like superoxide anion radicals, hydroxyl radicals, and hydrogen peroxide, are also the physiological byproduct of the aerobic metabolism that takes place in the mitochondria. ROS levels must be finely regulated by scavengers (e.g. glutathione peroxidase, thioredoxins, superoxide dismutase) that quickly process them into innocuous molecules[118]. Cancer cells are often in a hypoxic environment characterized by intense metabolic activity and consequent production of high levels of ROS, thus they must adapt to a constant condition of oxidative stress.

Although high levels of ROS are cytotoxic for both normal and cancer cells, balanced levels of ROS can promote tumorigenesis by inducing genetic and epigenetic instability[119].

In order to overcome all these stresses, tumor cells divert the mechanisms used by normal cells and adapt, activating the ER stress response pathways, ROS-scavenging systems and the oxidative

stress response, autophagy and inhibiting cell death factors normally leading to apoptosis in the presence of excessive stress.
Certainly, dynamism and reversibility are key features of these processes, the same as the m^6A RNA modification.
Recently, different works have highlighted the correlation between m^6A modification and several kinds of stress. In particular, as Wei et al. reported in their work, in liver disease, accumulation of misfolded/unfolded proteins selectively induces METTL14 expression, which in turn suppresses CHOP expression through m^6A methylation and consequently triggers CHOP mRNA degradation, selecting for stress adaptation over apoptosis in response to ER stress[120].

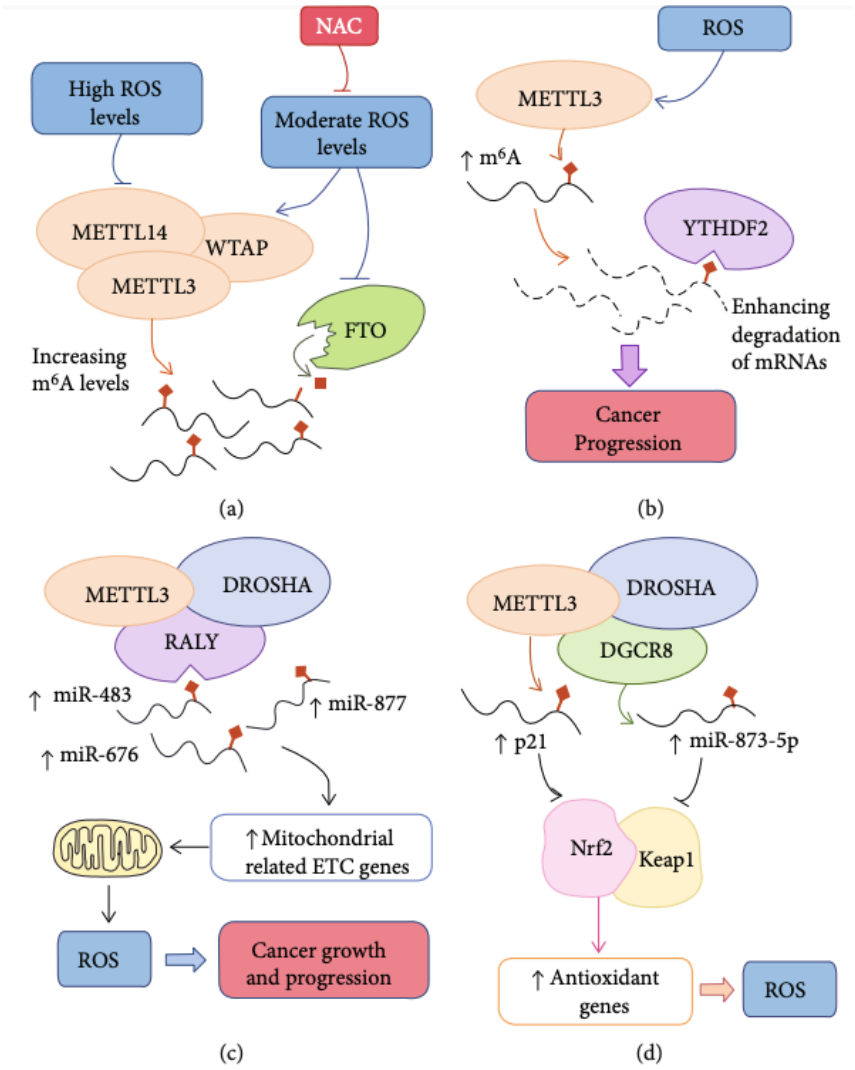

Figure 2.4. Interplay between ROS and m⁶A. (a and b) ROS influence m⁶A enzymes in a dose-dependent way: high ROS levels induce downregulation of METTL3, WTAP and METTL14, while moderate ROS levels have an opposite effect. (c and d) m⁶A modification on target mRNAs and miRNAs affects ROS production through mitochondrial related ETC gene and Nrf2/Keap1 pathway

It has been demonstrated that ROS levels can regulate m^6A enzymes and, therefore m^6A modification levels. In particular, Qui L. et al. and Zhao T. et al., have shown that oxidative stress induced by H_2O_2 or arsenite leads to increased protein levels of METTL3, METTL14 and WTAP. However, high doses of arsenite led to the opposite effect, to a lowering of protein levels of m^6A enzymes [121,122].
At the same time several research groups have shown that m^6A RNA modification can control redox homeostasis. The presence of the m^6A modification on pri-mir483, pri-mir877, and pri-mir676 promotes their binding to RALY and their processing, thus leading to downregulation of mitochondrion-related ETC (electron transport chain) genes and ROS production[123]. Another interesting work showed that METTL3-dependent maturation of miR-873-5p as well as p21 induction could activate the Nrf2 antioxidant pathway by inhibiting its negative regulator Keap1, to resist oxidative stress and apoptosis[124,121].
Also circRNAs may play an important role in cellular stress responses. Some of them are important for maintaining cellular homeostasis, while, dysregulation of others, could lead to tumor development and progression. Zhou et al., observed a negative correlation of circ_002117 with the degree of malignancy of gastric cancer. In fact, they showed that circ_002117, acting as a sponge of miR-370, upregulates the levels of GRP78, IRE1, eIF2α and CHOP facilitating ER stress-induced apoptosis[125]. On the other hand, also circCDR1as upregulates eIF2α by inducing ER stress in Oral Squamous Cell Carcinoma (OSCC), but this leads to increased cancer cells viability[126]. Thus, circRNAs can have different effects on the stress response in different contexts while activating the same pathways.
Of particular interest is circFOXO3, which is highly expressed in senescent cells, where it interacts with the anti-senescence proteins ID1 and E2F1 and the anti-stress proteins FAK and HIF1α. Negative regulation of the latter leads to cell senescence. The function of circFOXO3 is to sequester these important transcription factors and retain them in the cytoplasm. In particular, what they have shown is

that in the presence of high levels of circFOXO3, HIF1α induced by H_20_2 treatment, fails to translocate into the nucleus[127].
As mentioned above, autophagy is another very important cellular process to maintain homeostasis. It consists in degradation and recycling of malfunctioning cytoplasmic components and organelles in order to recover energy and molecules. Under stress condition, due to accumulation of misfolded proteins, as well as in condition of starvation, autophagy can be induced to restore cellular homeostasis[128]. Similarly, it can be exploited by tumor cells as an energy source to grow and proliferate[129]. Both m^6A and circRNAs regulate autophagy, in physiological and non-physiological processes. There are a lot of works highlighting the role of m^6A in regulating autophagy in cellular processes. For example, METTL3 negatively regulates autophagy, by affecting the stability of Autophagy Related Gene (ATG7), and promoting senescence in fibroblast-like synoviocytes (FLSs)[130]. Under hypoxia condition in hepatocellular carcinoma, HIF1α induces YTHDF1 expression, which in turn promotes translation of autophagy-related genes ATG2A and ATG14 in a m^6A-dependent manner[131].
Liang G. et al., investigated the role of circCDYL in breast cancer, where it is highly expressed and promotes autophagy, acting as a sponge for miR-1275 and consequently increasing the expression of autophagy-associated genes ATG7 and ULK1[132].
In light of what has been described so far, altering proteostasis may be a promising strategy to combat both solid[133] and hematological cancers[134]. In this respect, an important example is the use of the proteosome inhibitor, Bortezomib or Velcade, which was subsequently approved for the clinical use as a front-line treatment for multiple myeloma (MM) and mantle cell lymphoma (MCL)[135]. Proteosome inhibition, resulting in the accumulation of proteins that should be degraded, leads to ER stress, as well as oxidative stress and induction of autophagy. For all these reasons, Btz is an excellent candidate for the purpose of this thesis.

3. AIMS

Acute myeloid leukemia represents a group of blood neoplasms characterized by several chromosomal translocations and mutations that lead to tumor growth and progression. Numerous research groups have devoted themselves to the study of this ominous disease, with much progress being made in research and clinical trials, but the numbers of recurrences are still too high.

M^6A and circRNAs both play a role in the onset and progression of this disease. We have already discussed for example that the up-regulation of METTL3 and METTL14 leads to the proliferation of LSCs, that the high expression of FTO can lead to drug resistance and that some circRNAs are involved as well, one example being circPAN3.

Moreover, the role of cellular stress and in particular oxidative stress in cancer has been highlighted in recent years. Various studies have highlighted how the tumor cell exploit mechanisms to overcome stress and use them to its advantage to accumulate mutation and escape from cell death. There is a subtle balance between stress and cell death, our aim is to disrupt this balance in order to induce apoptosis in AML.

Since proteasome inhibition leads to several stress responses, we decided to investigate the role of the proteasome inhibitor Bortezomib (Btz) on m^6A enzymes expression and in particular its impact on the modulation of m^6A-dependent circRNAs expression. In order to understand the possible role of m^6A-modified circRNAs during stress responses induced by Btz, the main aims of this PhD thesis are:

1. Evaluation of m^6A enzymes expression and their functional characterization during stress responses

2. Identification of m^6A modified-circRNAs modulated during stress responses

3. Functional characterization of identified m^6A circRNAs

It is shown below a flowchart that schematically illustrates the experimental design followed.

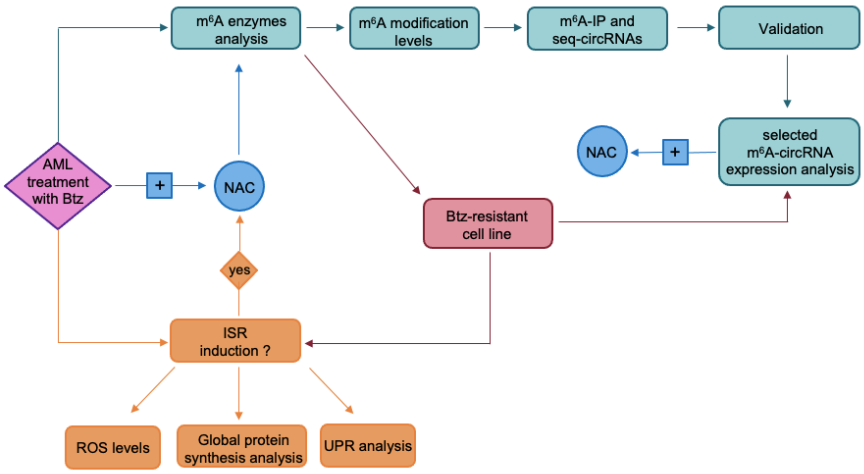

4. RESULTS

4.1 Btz treatment induces downregulation of m^{6}A enzymes expression at post-transcriptional level.

Since m^{6}A RNA modification has different roles in the biogenesis and function of circRNAs, and considering the involvement of cellular stress in malignant transformation, tumor progression and drug resistance[136,118], we decided to investigate the role of cellular stress induced by Btz on m^{6}A enzymes. Based on the data in literature and the dose-response curves already extensively analyzed in our laboratory, we decided to use two different doses of Btz at short times. We treated MOLM13, FLT3-ITD positive AML cell line, with 5nM and 10nM of Btz for 6h,16h and 24h in order to induce an acute stress. Cytofluorimetric analysis of cells stained by propidium iodide to assess cell death, shows that treatment with Btz at the indicated times and concentrations did not cause a high rate of cell death, with only 25-30% dead cells in the samples treated with the highest dose of Btz for 24h (Figure 4.1).

A

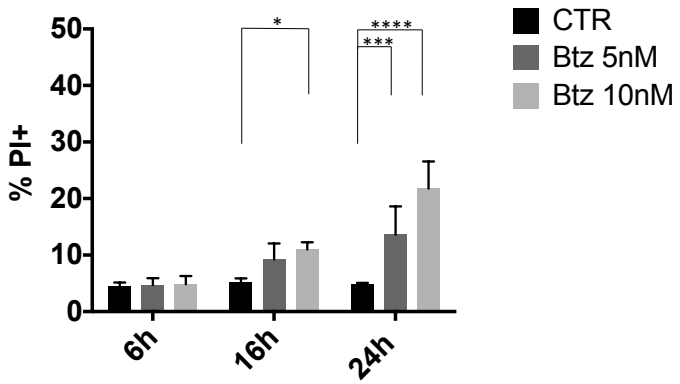

B

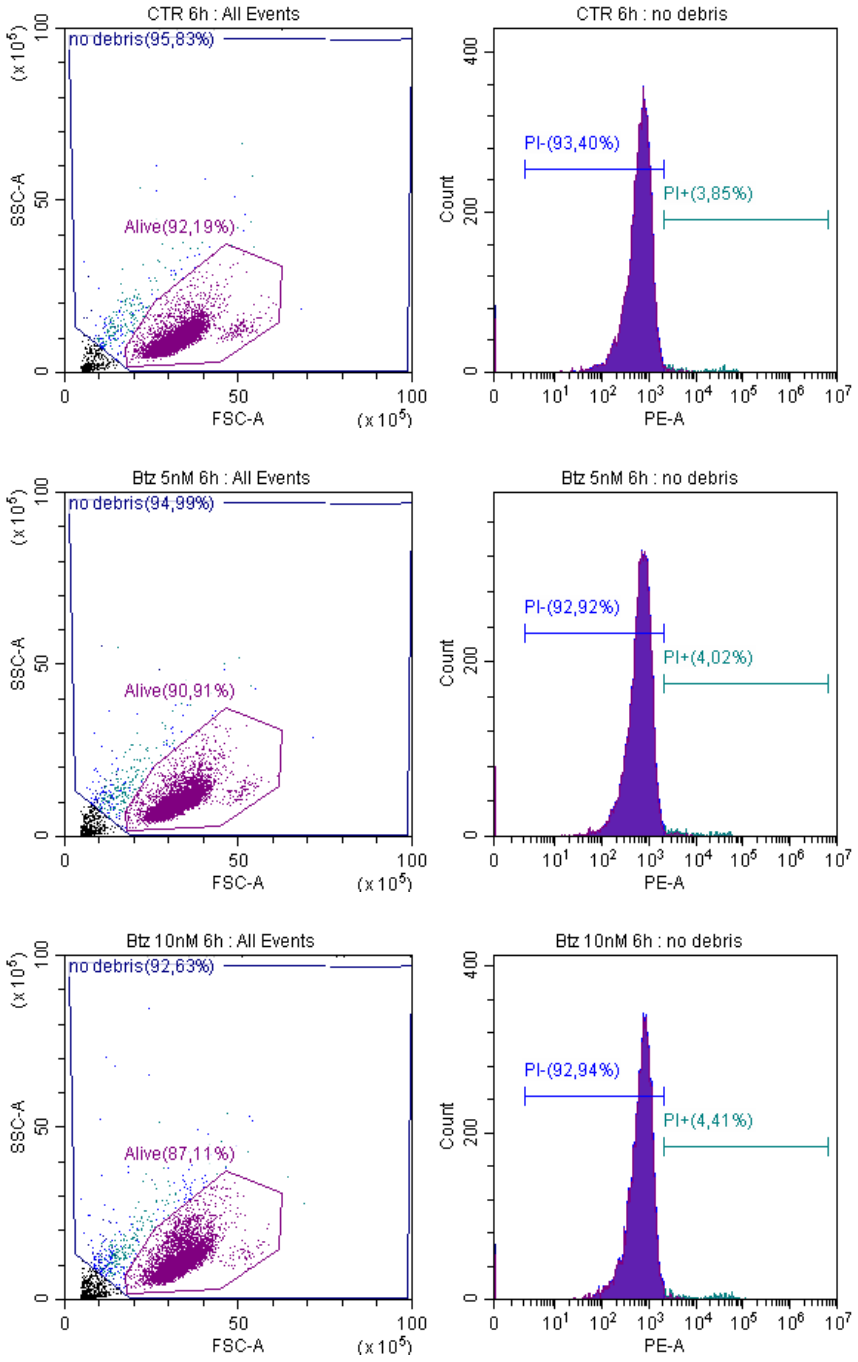
CTR 6h : All Events
no debris(95,83%)
Alive(92,19%)
SSC-A
FSC-A
CTR 6h : no debris
PI-(93,40%)
PI+(3,85%)
Count
PE-A
Btz 5nM 6h : All Events
no debris(94,99%)
Alive(90,91%)
Btz 5nM 6h : no debris
PI-(92,92%)
PI+(4,02%)
Btz 10nM 6h : All Events
no debris(92,63%)
Alive(87,11%)
Btz 10nM 6h : no debris
PI-(92,94%)
PI+(4,41%)

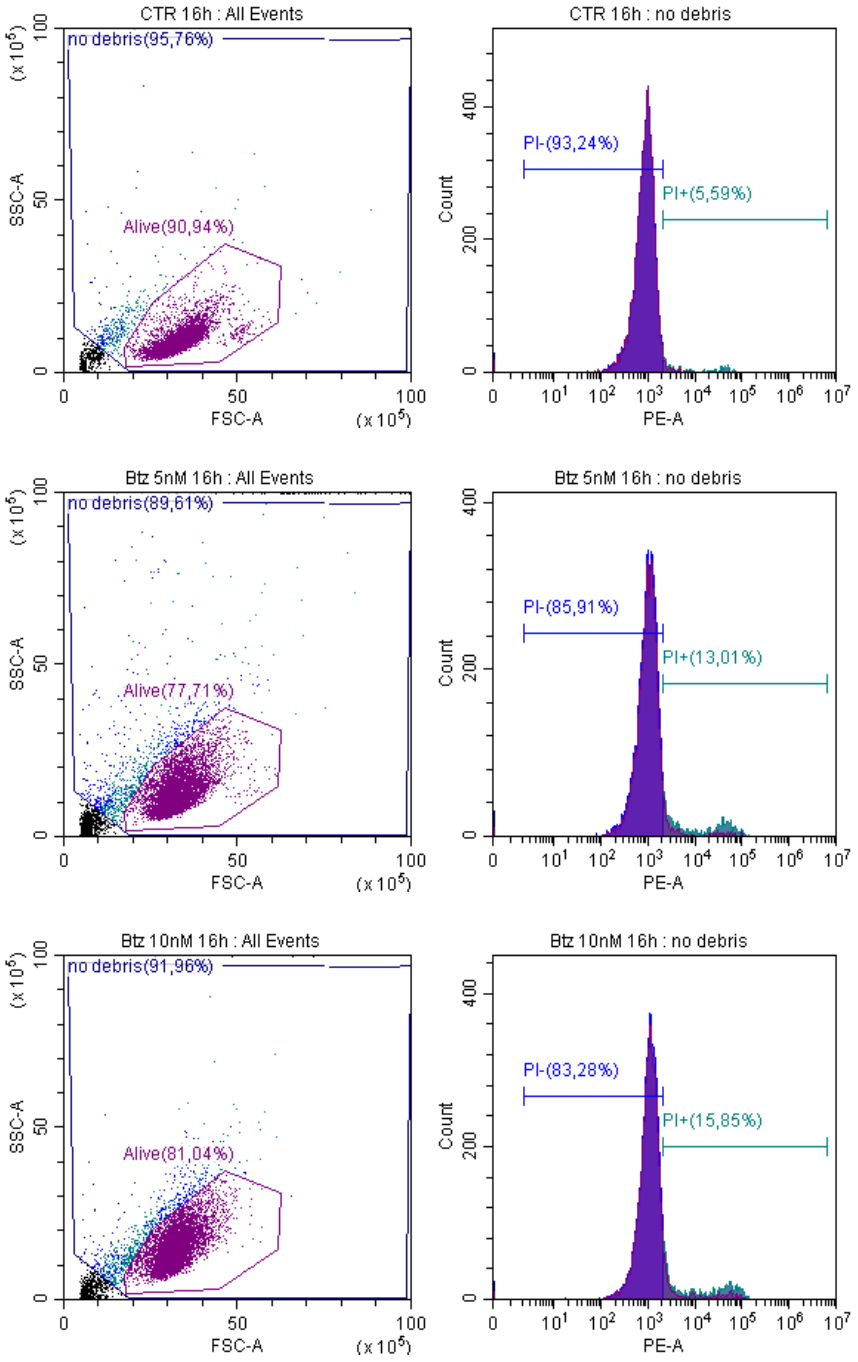
CTR 16h : All Events
no debris(95,76%)
Alive(90,94%)
SSC-A
FSC-A
(x 10^5)
CTR 16h : no debris
PI-(93,24%)
PI+(5,59%)
Count
PE-A
Btz 5nM 16h : All Events
no debris(89,61%)
Alive(77,71%)
Btz 5nM 16h : no debris
PI-(85,91%)
PI+(13,01%)
Btz 10nM 16h : All Events
no debris(91,96%)
Alive(81,04%)
Btz 10nM 16h : no debris
PI-(83,28%)
PI+(15,85%)

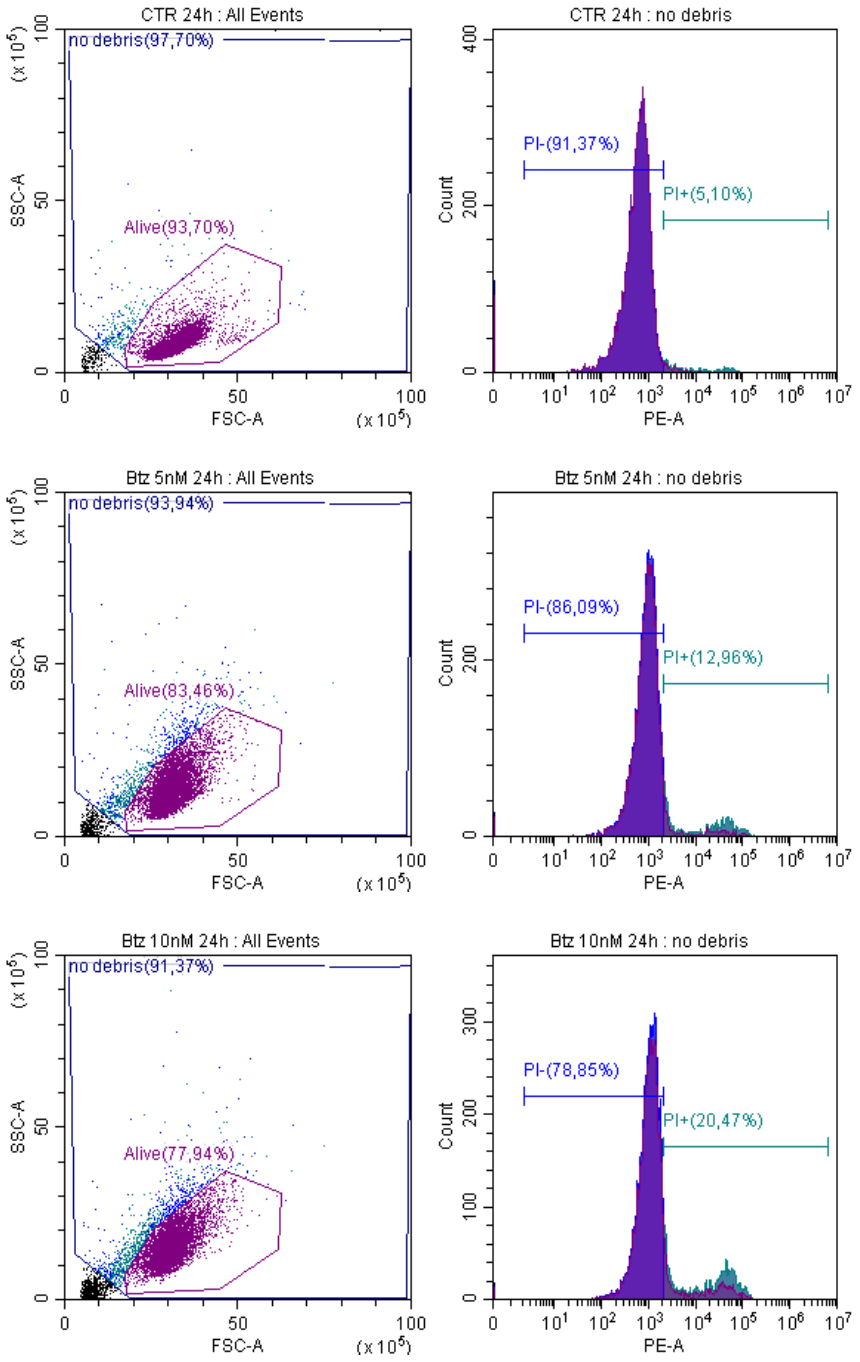
CTR 24h : All Events
no debris(97,70%)
Alive(93,70%)
SSC-A
FSC-A
(x 10^5)
CTR 24h : no debris
PI-(91,37%)
PI+(5,10%)
Count
PE-A
Btz 5nM 24h : All Events
no debris(93,94%)
Alive(83,46%)
Btz 5nM 24h : no debris
PI-(86,09%)
PI+(12,96%)
Btz 10nM 24h : All Events
no debris(91,37%)
Alive(77,94%)
Btz 10nM 24h : no debris
PI-(78,85%)
PI+(20,47%)

Figure 4.1. A. Percentage of cell death detected by propidium iodide (PI). **B** Representative images of the populations from cytofluorimetric analysis with the various treatments. N=4 *P≤0.05; ***P≤0.0005; ****P≤0.00005; statistical analysis was performed by Two-Way ANOVA.

We them moved to investigate the expression levels of some of the enzymes involved in m^6A RNA modification under acute stress conditions in AML. In particular, we analyzed the expression of the methyltransferase METTL3, the main player of this modification, together with the cofactor WTAP and the demethylase FTO. As shown in Figure 4.2A, we observed a general downregulation of the writer and its cofactor, METTL3 and WTAP, but also a decrease of the eraser FTO upon Btz treatment after 24h in MOLM13 cells. Interestingly, we saw a strong and significant decrease of WTAP protein expression levels, already at 16h of treatment and with the lowest Btz concentration, 5nM.
Next, we wondered about the effect of Btz on the reader enzymes of m^6A. We analyzed the protein expression levels of YTHDF2, a cytoplasmic reader involved in the degradation of messenger RNA, and YTHDC1, a nuclear reader with a splicing regulatory function. We did not observe significant deregulation of YTHDF2, whereas we found that YTHDC1 was downregulated as the other enzymes (Figure 4.2B).
In order to better understand if this regulation is transcriptional or post-transcriptional, we decided to investigate this molecular aspect further by evaluating the RNA levels of the same m^6A enzymes analyzed in terms of protein expression by RT-qPCR. As it can be seen in Figure 4.3, we didn't observe down-regulation at transcriptional level, suggesting post-transcriptional regulation of these enzymes upon Btz treatment.

A

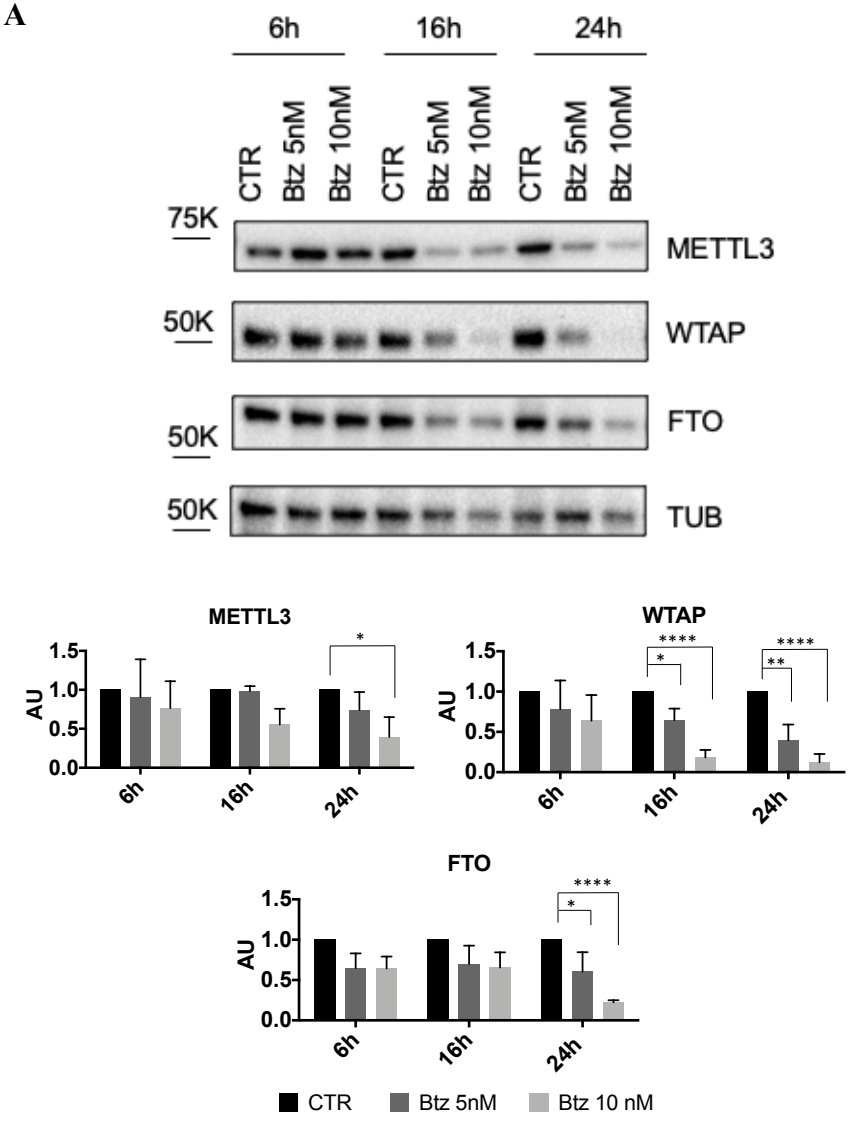
6h
16h
24h
CTR
Btz 5nM
Btz 10nM
75K
METTL3
50K
WTAP
50K
FTO
50K
TUB
METTL3
WTAP
FTO
AU
1.5
1.0
0.5
0.0
6h
16h
24h
*
****
**
CTR
Btz 5nM
Btz 10 nM

B

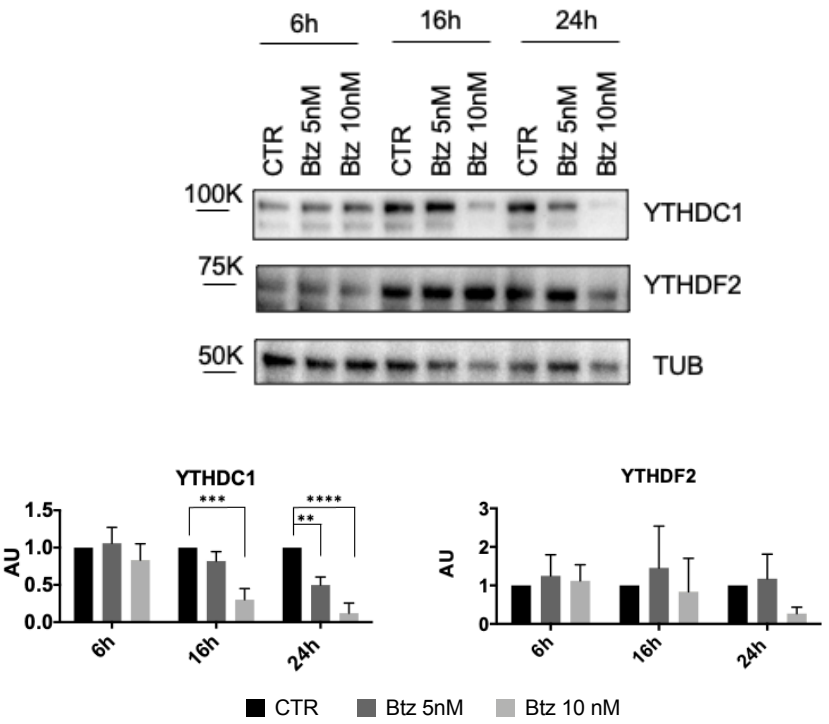

Figure 4.2. A. Representative western blot of METTL3, WTAP and FTO with relative quantification **B.** Representative western blot of YTHDF2 and YTHDC1 and relative quantification. N=4 *P≤0.05; **P≤0.005; ***P≤0.0005; ****P≤0.00005; statistical analysis was performed by Two-Way ANOVA.

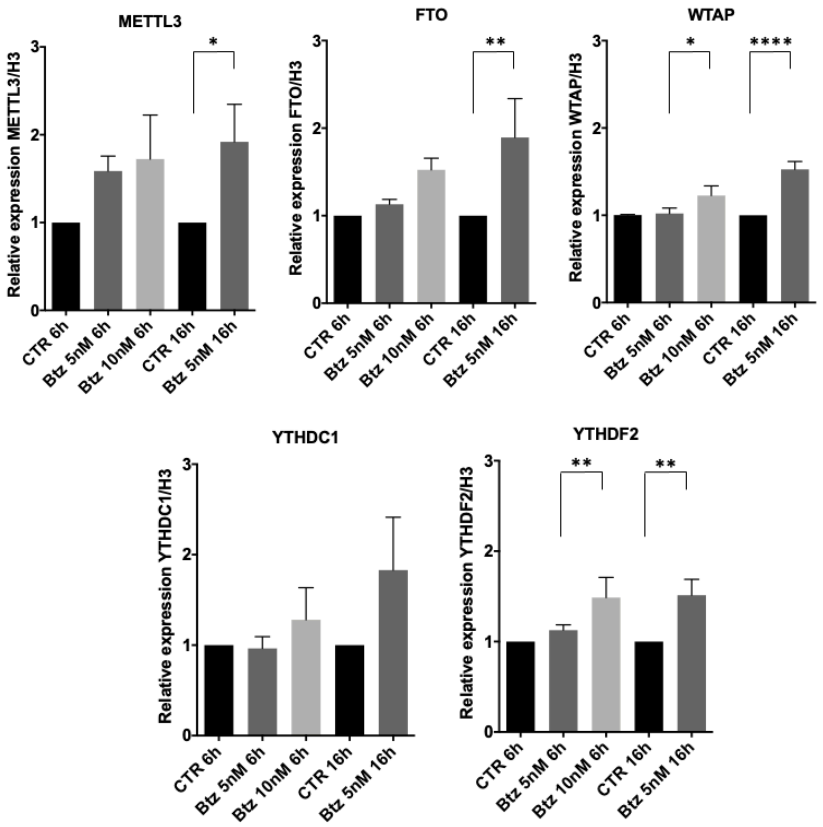

Figure 4.3. RT-qPCR analysis of WTAP, FTO, METTL3, YTHDF2 and YTHDC1 mRNA expression after 6h of treatment with 5nM and 10nM of Btz, and after 16h of treatment with 5nM of Btz. N=4 *P≤0.05; **P≤0.005; ***P≤0.0005; statistical analysis was performed by Two-Way ANOVA

4.2 Btz treatment induces inhibition of global translation.

In accordance with data from literature, intrinsic and extrinsic conditions like ER Stress, hypoxia, oxidative stress and proteasome inhibition lead to activation and phosphorylation of eIF2α, which causes global inhibition of protein synthesis[137].
For this reason, we wondered whether the depletion of the majority of m^6A enzymes was due to a decrease of global protein synthesis. To address this question, we performed a translation assay based on puromycin, a tyrosyl-tRNA mimic that blocks translation by labeling and releasing elongating polypeptide chains from translating ribosomes. In particular, control cells and cells treated with Btz 5nM and 10nM were challenged with puromycin for 0, 10 o 30 minutes and then we measured the levels of newly synthesized polypeptides using an anti-puromycin antibody. As represented in Figure 4.4, we observed a strong decrease of puromycin incorporation upon Btz treatment, particularly evident with the highest concentration compared to control cells, indicating a global decrease of protein synthesis. This finding is in agreement with the observations relative to the clear drop in protein levels of m^6A enzymes after 24h treatment with Btz 10nM.
In order to understand if the strong decrease of these enzymes depends on translation or on protein destabilization, we performed a Cycloheximide (CHX) chase assay, used to measure steady state protein stability. After 16h h of 5nM Btz treatment we treated cells with CHX for 0h (our control cells without CHX),1h and 3h. Intriguingly, after cycloheximide treatment, METTL3 and FTO protein levels didn't decrease, while WTAP protein decreased significantly already after 1h of CHX treatment, almost disappearing after 3h of treatment. This data leads us to hypothesize that treatment with Btz 5nM induces a strong destabilization of WTAP and that it has a very short half-life (Figure 4.5).

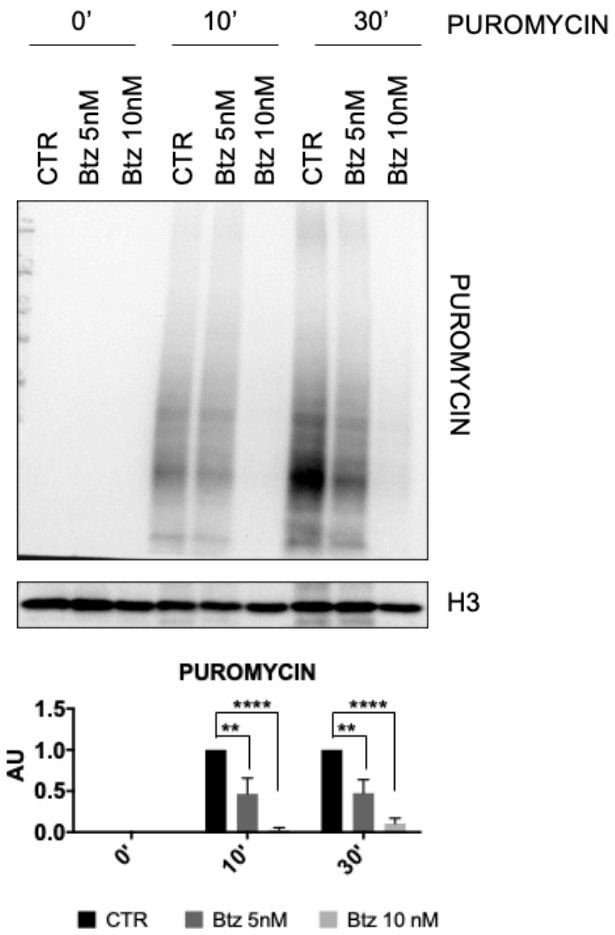

Figure 4.4. Detection by western blot analysis of puromycin incorporation after 0', 10' and 30' in control cells and in cells treated with Btz 5nM for 16h. On the bottom is presented the quantification relative to the control for each time point. **P≤0.005; ****P≤0.00005; statistical analysis was performed by Two-Way ANOVA

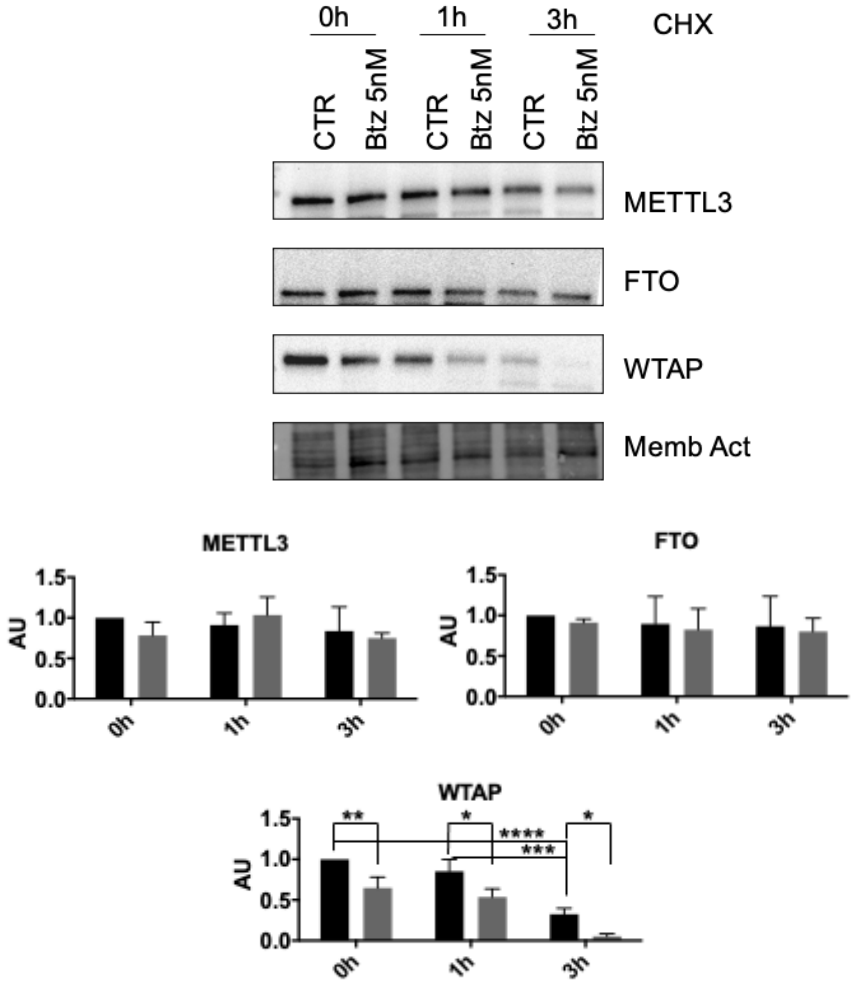

Figure 4.5. Representative Western blot analysis of MOLM13 cells treated with 5Nm of Btz for 16h and subsequently with CHX for additional 0h (CHX -), 1h and 3h. On the bottom, relative quantification of METTL3, FTO and WTAP protein levels, normalized on total protein measured by stain-free BioRad method. *P≤0.05; **P≤0.005; ***P≤0.0005; ****P≤0.00005; statistical analysis was performed by Two-Way ANOVA.

4.3 Btz treatment induces the Integrated Stress response (ISR).

As mentioned above, several cellular stresses can activate ISR by phosphorylating eIF2α and impairing global translation efficiency. Since we observed a strong decrease of global protein synthesis, we decided to investigate whether Btz treatment induced ISR by assessing the levels of eIF2α phosphorylation. As can be seen in Figure 4.6, treatment with Btz determined an increase in the phosphorylated form of eIF2α, particularly significant after 16h and 24h at the lowest concentration, indicating that the doses of Btz used, induced the ISR. Moreover, we observed an increase of BiP protein upon Btz treatment, indicating the presence ER stress likely generated by the accumulation of misfolded proteins due to proteasome inhibition.

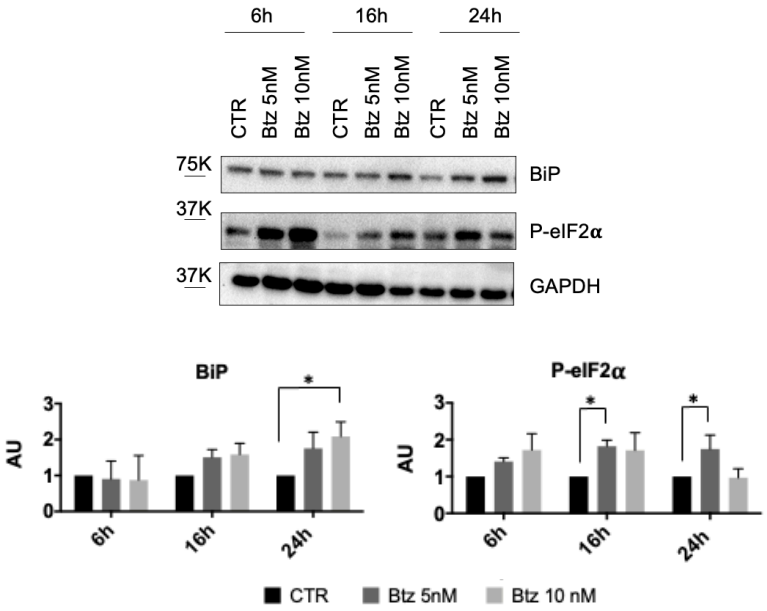

Figure 4.6. Representative Western blot analysis of BiP and P-eIF2α in MOLM13 cells treated with 5nM and 10nM of Btz for 6, 16 and 24h. On the bottom relative quantification. N=4 *P≤0.05; **P≤0.005; ***P≤0.0005; ****P≤0.00005; statistical analysis was performed by Two-Way ANOVA.

As described in the introduction, under ER stress condition, the oxidative folding of proteins, and thus the formation of disulphide bonds, can occur in a dysregulated manner and lead to accumulation of reactive oxygen species, causing oxidative stress. Therefore, we wondered whether treatment with Btz could induce also oxidative stress. To address this, we measured, by cytofluorimetric analysis, the amount of ROS 3h and 6h after Btz treatment. As you can see in Figure 4.7, we observed an accumulation of ROS after 3h and 6h with the highest concentration of Btz, 10nM. Furthermore, as confirmation of these data we observed an increase in transcriptional levels of heme oxygenase-1 (HMOX-1), one of the genes activated in the antioxidant response.

A

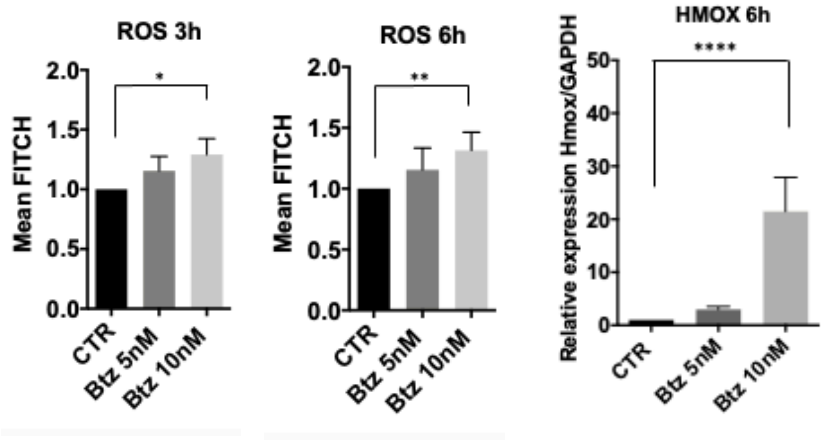

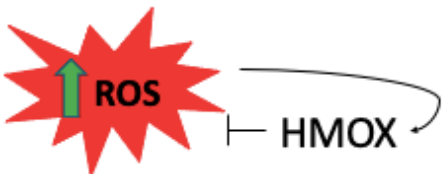

B

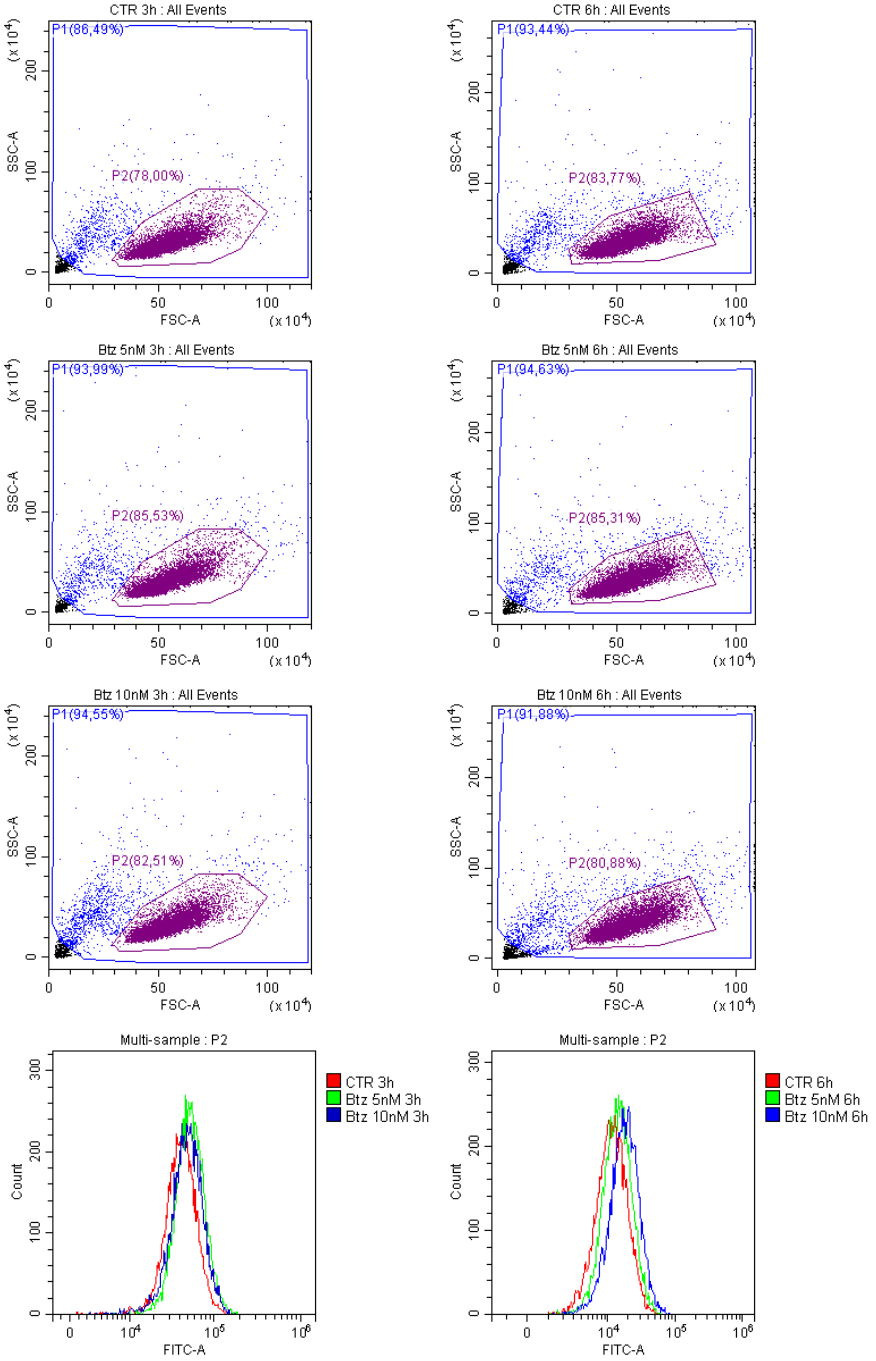
CTR 3h : All Events
P1(86,49%)
P2(78,00%)
CTR 6h : All Events
P1(93,44%)
P2(83,77%)
Btz 5nM 3h : All Events
P1(93,99%)
P2(85,53%)
Btz 5nM 6h : All Events
P1(94,63%)
P2(85,31%)
Btz 10nM 3h : All Events
P1(94,55%)
P2(82,51%)
Btz 10nM 6h : All Events
P1(91,88%)
P2(80,88%)
SSC-A
FSC-A
(x10⁴)
Multi-sample : P2
Count
FITC-A
CTR 3h
Btz 5nM 3h
Btz 10nM 3h
CTR 6h
Btz 5nM 6h
Btz 10nM 6h

Figure 4.7. A Cytofluorimetric detection of ROS after 3h and 6h of Btz treatment by using oxidized DCF-DA (on the left panel). On the right RT-qPCR analysis of HMOX after 6h of 5nM and 10nM of Btz. **B** Representative images of the populations from cytofluorimetric analysis with the various treatments. N=4 *P≤0.05; **P≤0.005; ***P≤0.0005; ****P≤0.00005; statistical analysis was performed by Two-Way ANOVA.

To understand if m^6A enzymes deregulation induced by Btz was due to the high levels of ROS, we decided to treat cells with N-acetylcysteine (NAC). NAC is one of the compounds most widely used as a pharmacological antioxidant and cytoprotectant. In particular, one day in advance to Btz treatment, we administrated NAC to MOLM13 cells or water (control sample). After 16h of Btz treatment, in the samples treated with NAC, we observed a recovery of m^6A enzyme protein expression levels, particularly significant for WTAP, suggesting that m^6A proteins decrease may be due to oxidative stress (Figure 4.8A). Moreover, in the same experimental conditions we performed RT-qPCR analysis of Hmox, that showed levels of expression similar to the control samples as reported in Figure 4.8B).

A

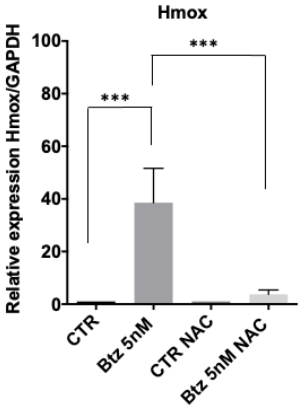
Hmox
Relative expression Hmox/GAPDH
100
80
60
40
20
0
***
***
CTR
Btz 5nM
CTR NAC
Btz 5nM NAC

B

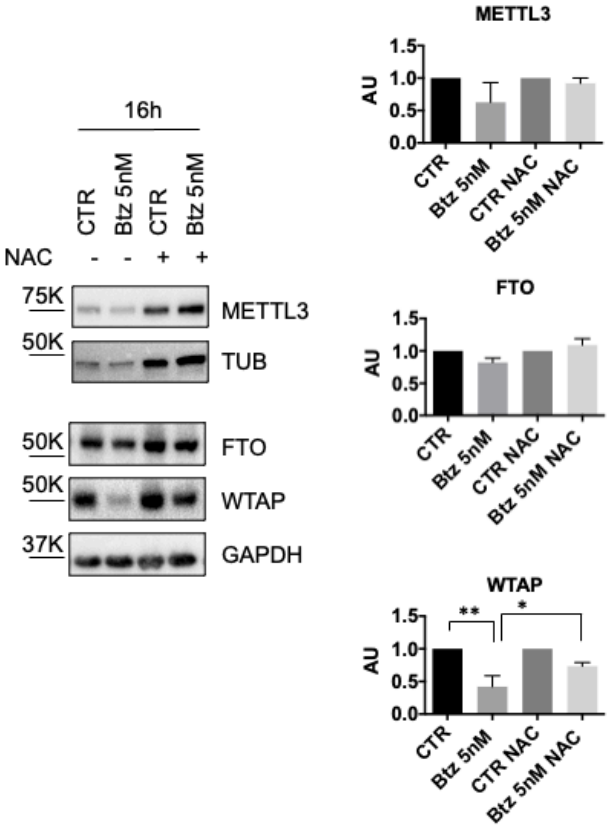
16h
CTR
Btz 5nM
CTR
Btz 5nM
NAC - - + +
75K
METTL3
50K
TUB
50K
FTO
50K
WTAP
37K
GAPDH
METTL3
AU
1.5
1.0
0.5
0.0
CTR
Btz 5nM
CTR NAC
Btz 5nM NAC
FTO
AU
1.5
1.0
0.5
0.0
CTR
Btz 5nM
CTR NAC
Btz 5nM NAC
WTAP
AU
**
*
1.5
1.0
0.5
0.0
CTR
Btz 5nM
CTR NAC
Btz 5nM NAC

Figure 4.8. A. Representative Western blot of METTL3, FTO and WTAP after 16h of Btz treatment, in presence or not of NAC and relative quantification. **B.** RT-qPCR analysis of Hmox in the same condition. N=4 *P≤0.05; **P≤0.005; ***P≤0.0005; statistical analysis was performed by Two-Way ANOVA.

4.4 Btz treatment induces downregulation of global m^{6}A modification levels

Since we observed a general decrease in m^{6}A enzyme protein levels, both writers and erasers, we wondered about the effect of Btz-induced stress on the general m^{6}A modification levels. To address this question, we treated MOLM13 cell line with 5nM of Btz for 16h and then analyzed the amount of m^{6}A through immunofluorescence by quantifying the fluorescence intensity. As you can see in Figure 4.9, while in the control we have many cells with an intense green coloration, indicative of strong m^{6}A RNA methylation, in the Btz-treated cells, the fluorescence intensity, and therefore methylation level, is reduced.

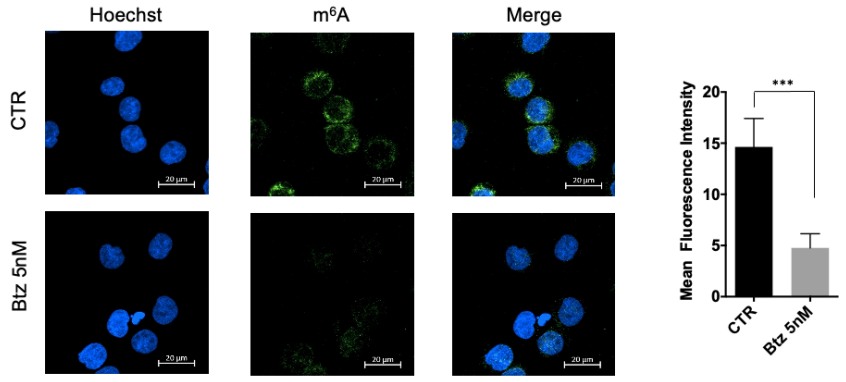

Figure 4.9. MOLM13 treated with 5nM of Btz for 16h, labeled with DAPI (cell nuclei) and with anti-m^{6}Ab labeled with Alexa Fluor 488 (m^{6}A modification). Scale bars, 20 µm. N=3 ***P≤0.0005; statistical analysis was performed by T-Test.

4.5 Identification of m^{6}A-modified circRNAs modulated upon Btz treatment

As mentioned, among our aims there is the identification of m^{6}A modified circRNAs differentially expressed upon proteotoxic stress. Once we assessed that Btz alters m^{6}A levels we performed m^{6}A-Immunoprecipitation (m^{6}A-IP) on the samples treated with 5nM of Btz for 16h. In detail, we isolated total RNA, treated it with RNaseR to remove all the linear RNA and the majority of ribosomal RNA, and proceeded with m^{6}A-IP. M^{6}A-immunoprecipitated RNAs from CTR- and Btz- treated cells were then analyzed by RNAseq (Figure 4.10A). To select circRNA deregulated between CTR and Btz-treated MOLM13 cells, we considered those circRNAs that were expressed (CPM value>0) in all the considered anti-m^{6}A-immunoprecipitated samples (replicates #1 and #7). By filtering circRNAs showing modulation in both biological replicates (Fold Btz vs CTR >1.5 or <0.75) we identified 47 up regulated and 8 down regulated circRNAs. Five circRNAs (Table 1) were selected, based on their high expression level, for further validation and functional characterization.

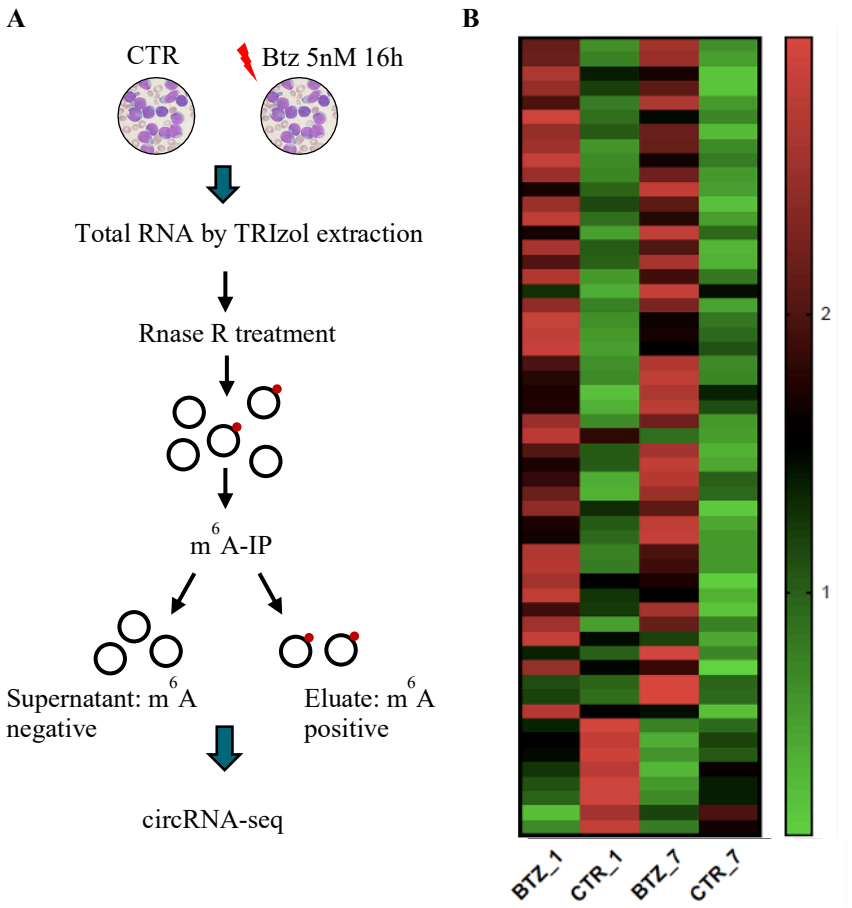

Figure 4.10 A. Schematic representation of Btz treatment followed by m^{6}A-IP. **B.** Expression matrix showing the circRNAs identified by m^{6}A-IP-RNAseq, as up-regulated or down-regulated in MOLM13 cells treated with Bortezomib vs control untreated cells followed by m^{6}A-IP. Fold cut-off=1.5. Expression values are presented as z-scores. N=2

We first interrogated circbank[138] repository to analyze the genomic organization of the selected circRNAs. We observed that circZNF609 (874bp), circHIPK3 (1099bp) and circRNF220 (742bp) all derive from the exon 2 of their hosting genes (Figure 4.11). On the contrary, circAFF1 and circSATB1 are multi-exonic circRNAs. In particular, circAFF1 (1021bp) derives from exons 3 and 4 of the AFF1 gene, while circSATB1 (1599bp) contains exons 3 to 10 of SATB1 gene (Figure 4.11).
To validate the bioinformatic analysis of RNAseq, we performed additional biological replicates of the m^{6}A immunoprecipitation in the same experimental condition (Btz 5nM for 16h), but without performing RNAseR treatment. We then analyzed these samples by RT-qPCR using divergent primers that recognize the splicing junction of the selected circRNAs (indicated in Table 1).
As shown in Figure 4.12, circZNF609, circHIPK3, circRNF220 and circAFF1 were all significantly hypermethylated after treatment with Btz, compared to control sample, while circSATB1 showed a trend of up-regulation, but didn't reach the statistical significance.

Table 1. CircRNAs identified by m^{6}A-IP-RNAseq and selected for validation experiments

circ_coordinates (HOST GENE)	BTZ#1 (cpm)	BTZ#7 (cpm)	CTR#1 (cpm)	CTR#7 (cpm)	Fold#1 (cpm)	Fold#7 (cpm)
chr15:64791492|64792365 (ZNF609)	17,095	15,183	11,851	7,684	1,443	1,976
chr1:44877653|44878394 (RNF220)	11,011	7,971	7,008	3,375	1,571	2,362
chr11:33307959|33309057 (HIPK3)	13,453	15,183	7,330	7,244	1,835	2,096
chr4:87967318|87968746 (AFF1)	12,896	14,500	6,443	5,571	2,002	2,603
chr3:18419662|18462483 (SATB1)	14,396	20,801	10,269	8,973	1,402	2,318

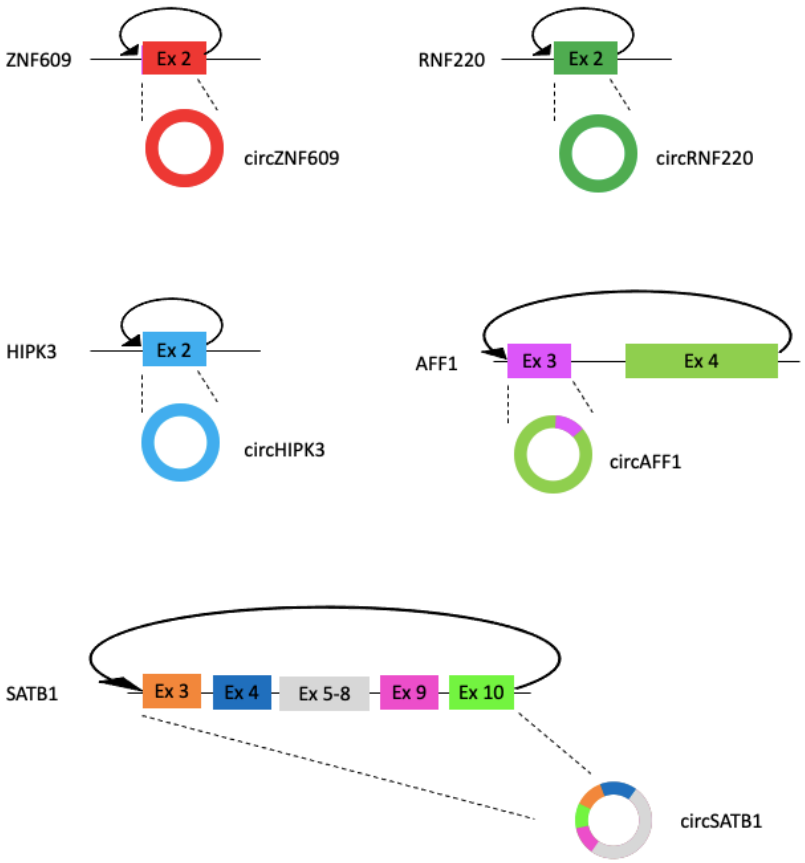

Figure 4.11. Schematic representation of genomic structure of circZNF609, circRNF220, circHIPK3, circAFF1, circSATB1.

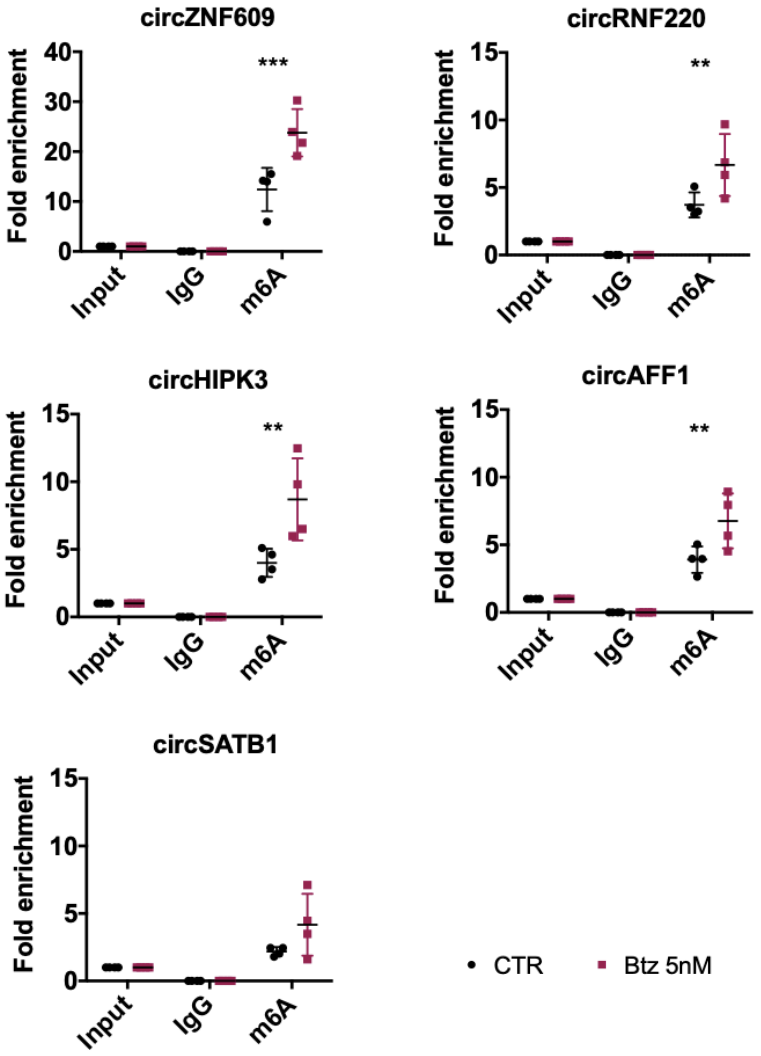

Figure 4.12. RT-qPCR analysis of circZNF609, circRNF220, circAFF1, circHIPK3 and circSATB1 in control and Btz-treated samples after m^6A-IP. N=4 **P≤0.005; ***P≤0.0005; statistical analysis was performed by Two-Way ANOVA.

4.6 Btz-resistant clones are able to control oxidative stress

Since these circRNAs are hypermethylated in a context of general hypomethylation, we wondered whether they could play a key role in the Btz response. Consequently, we generated MOLM13 Btz resistant cell line in order to study their expression.
In particular, as reported also in the schematic Figure 4.13A, we treated MOLM13 cell line with increasing doses of Btz every 4 weeks, changing the medium every 4 days. After three months of treatment, we seeded the cells in 96-wells in serial dilution and we isolated the single resistant clones (subclones). In total, we managed to isolate 3 different Btz-resistant clones, on which we started to perform functional assays.
In the first instance, we confirmed that our lines had actually become resistant to Btz by treating them with both 5nM and 10nM concentration, for longer than 72h. We also treated the parental MOLM13 cell line in the same conditions. After 72h of treatment, we performed a cytofluorimetric analysis of cell death upon propidium iodide uptake. As you can see in Figure 4.13B after 72 hours of treatment with 5nM of Btz there was no cell death in the clone cultures. We found 50% cell death with 10nM Btz, that still indicate resistance if we compare these results with those obtained with the parental MOLM13 cell line, which resulted in 100% cell death upon treatment with both concentrations. The clone that responded best to the treatments was the clone 3, so from here on we will show only the functional analysis on this one.

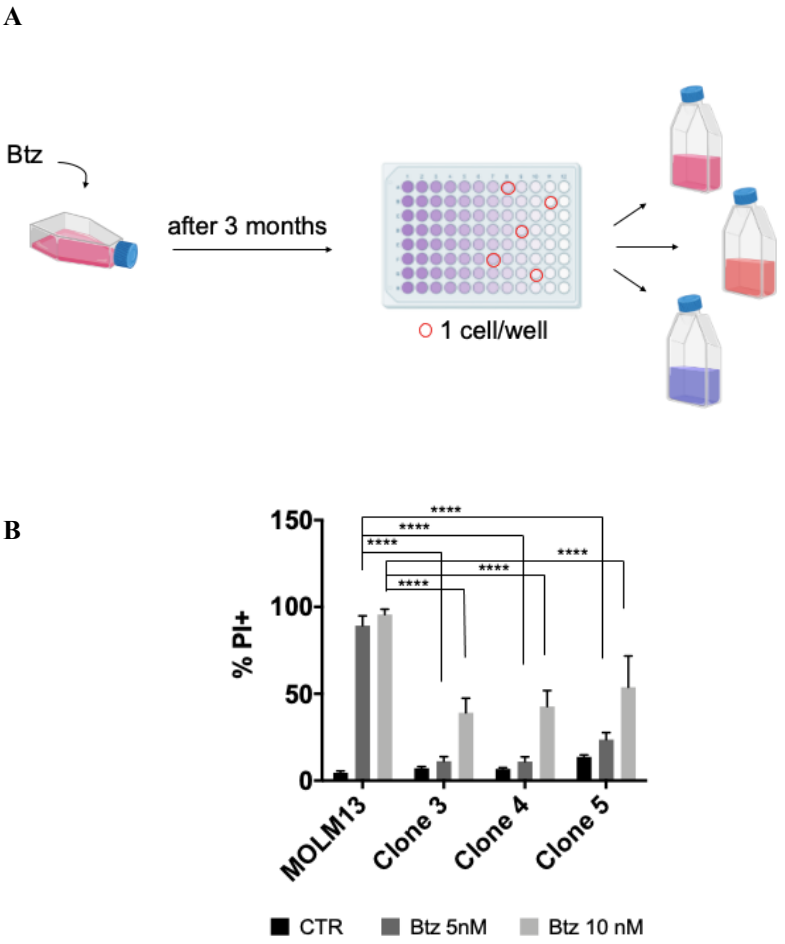

Figure 4.13.A. Schematic representation of clones' selection. **B.** Cytofluorimetric analysis of cell death detected by propidium iodide exclusion assay. N=4, ****P≤0.00005; statistical analysis was performed by Two-Way ANOVA.

As Btz treatment in MOLM13 cells induced down-regulation of protein expression of some methyltransferase complex components, particularly evident for WTAP, we investigated their expression in the Btz-resistant clone 3 under the same experimental conditions, Btz 5nM and 10nM for 6, 16 and 24h. As can be seen from the western blot in Figure 4.14, the Btz-resistant clone 3 no longer showed downregulation of the m^6A enzymes relative to control samples.
At this point, having previously observed stress induction resulting in ISR activation, we wondered about the Btz-induced stress response of this clone. To address this, we analyzed P-eIF2α protein, which showed a slight, but non-significant, increase, while BiP protein expression level remained constant in a dose and time-depended manner.

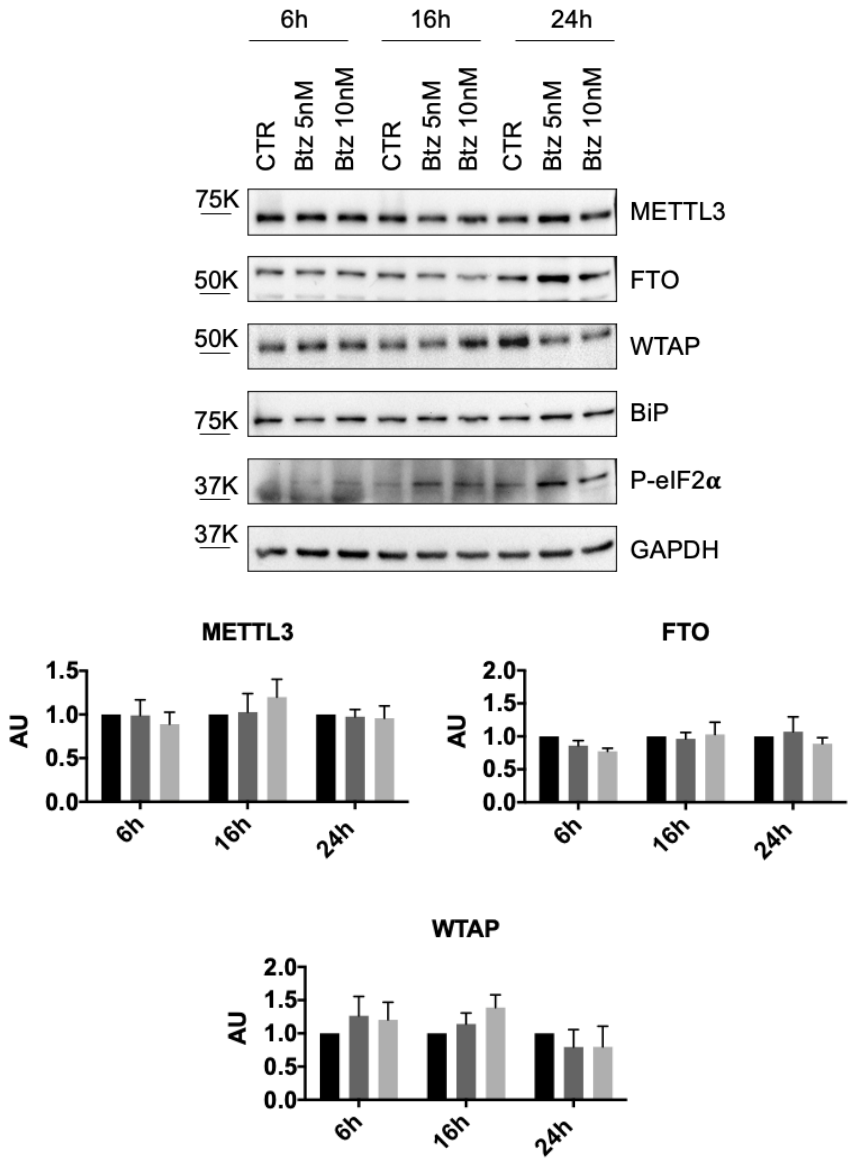
6h
16h
24h
CTR
Btz 5nM
Btz 10nM
CTR
Btz 5nM
Btz 10nM
CTR
Btz 5nM
Btz 10nM
75K
METTL3
50K
FTO
50K
WTAP
75K
BiP
37K
P-eIF2α
37K
GAPDH
METTL3
AU
1.5
1.0
0.5
0.0
6h
16h
24h
FTO
AU
2.0
1.5
1.0
0.5
0.0
6h
16h
24h
WTAP
AU
2.0
1.5
1.0
0.5
0.0
6h
16h
24h

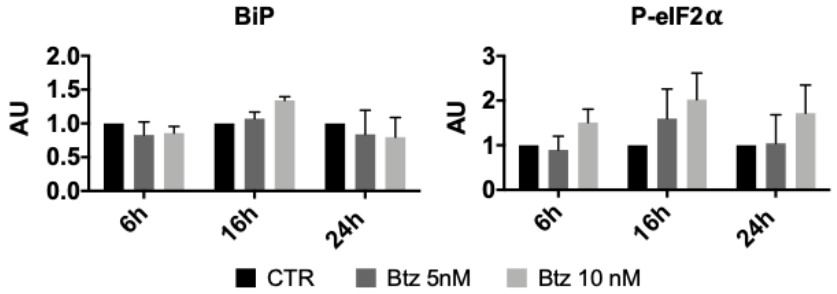

Figure 4.14. Representative western blot of METTL3, WTAP, FTO, BiP and P-eIF2α with relative quantification in Btz resistant clone 3, treated with 5nM and 10nM of Btz for 6,16 and 24h. N=3 statistical analysis was performed by Two-Way ANOVA.

In order to evaluate Btz-induced oxidative stress in Btz-resistant cells, we analyzed the amount of ROS in clone 3 treated with 5nM and 10nM Btz for 3 and 6h. As shown in Figure 4.15, there were no significant changes comparing treated and control sample, in all the experimental conditions. On the other hand, the difference in ROS detection was significant between parental MOLM13 samples treated with Btz compared to the clone 3. In fact, after 6h of stress induced by the highest concentration of Btz, we found activation of the antioxidant response as evidenced by increased levels of Hmox mRNA, but still at lower levels than those induced in wild type cell line.
All together these data suggest that Btz treatment induced a certain degree of stress, but Btz resistant cells are nevertheless able to keep it under control.

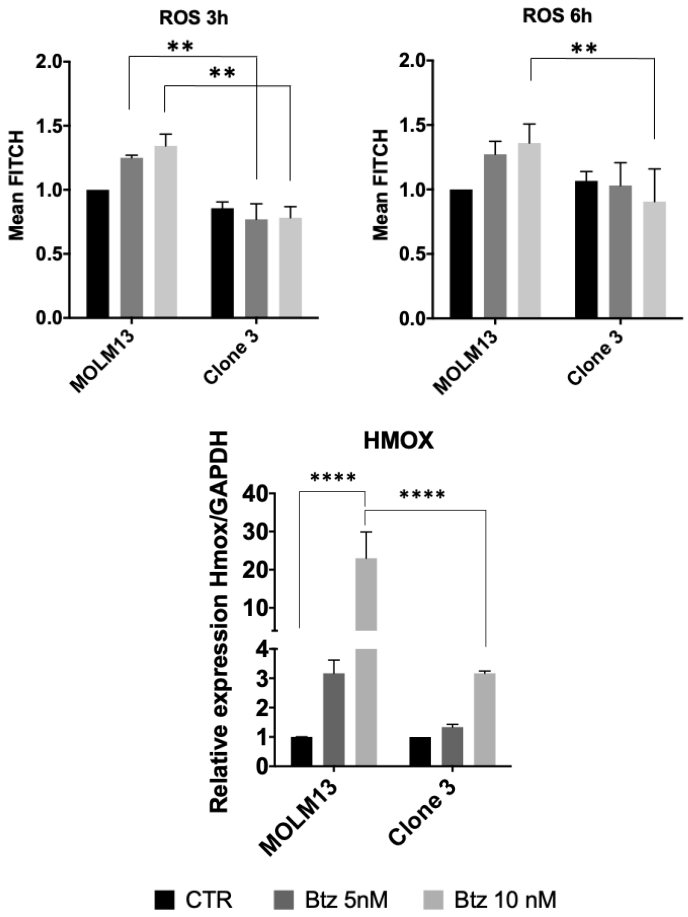

Figure 4.15. ROS detection after 3h and 6h of Btz treatment in MOLM13 cell line and Btz-resistant clone 3, by cytofluorimetry. On the bottom RT-qPCR analysis of Hmox in the same samples treated with Btz for 6h, as described above. N=4 **P≤0.005; ****P≤0.00005 statistical analysis was performed by Two-Way ANOVA.

4.7 Btz-dependent m^{6}A-modified circRNAs induction is impaired in Btz resistant cells

Once we identified m^{6}A-modified circRNAs modulated upon Btz treatment, we wondered how their expression changed in MOLM13 parental cell line and Btz-resistant clone 3 upon treatment, to investigate their role in the Btz-induced stress response. To address this question, we treated MOLM13 and Btz-resistant clone 3 with 5nM Btz for 16h and then we analyzed the expression of the selected circRNAs (see paragraph 4.5) by RT-qPCR. As it can be seen in Figure 4.15, we saw a significant up-regulation of the five selected m^{6}A-modified circRNAs that resulted hypermethylated upon Btz treatment by sequencing in MOLM13 cell line. Interestingly, the up-regulation of circZNF609, circRNF220, circHIPK3 and circSATB1 upon treatment with Btz was reduced in Btz-resistant clone 3 in the same experimental conditions, as well as that of circAFF1 although not significantly.
These data suggest that Btz treatment induced not only an increase in the methylation levels of the selected circRNAs, but also an increase in their expression.
Since we observed an increase in ROS levels following Btz treatment, and since oxidative stress plays an important role on the protein expression levels of m^{6}A enzymes, especially on WTAP (see paragraph 4.1), we wanted to investigate the expression levels of the selected circRNAs in response to Btz under reducing conditions.
We therefore treated MOLM13 with Btz 5nM in the presence or not of NAC. As shown in Figure 4.16, the expression of the selected circRNAs increased in the samples treated with Btz, as previously demonstrated, whereas it did not change in the samples pretreated with NAC before treatment with Btz. This suggests that the selected circRNA, hypermethylated upon Btz treatment, are dependent on oxidative stress and may play a role in modulating Btz-induced stress.

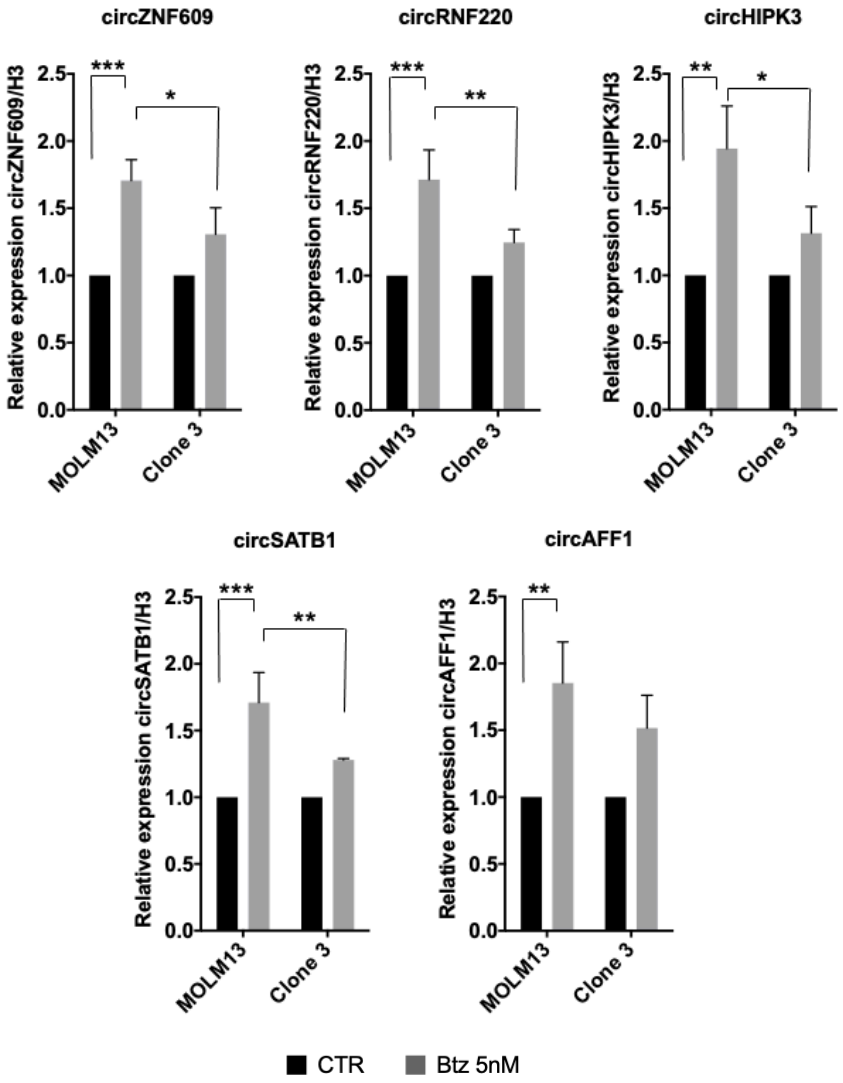

Figure 4.16. RT-qPCR analysis of circZNF609, circRNF220, circAFF1, circHIPK3 and circSATB1 in control and Btz-treated samples in MOLM13 and in Btz-resistant clone 3. N=4 *P≤0.05; **P≤0.005; ***P≤0.0005; statistical analysis was performed by Two-Way ANOVA.

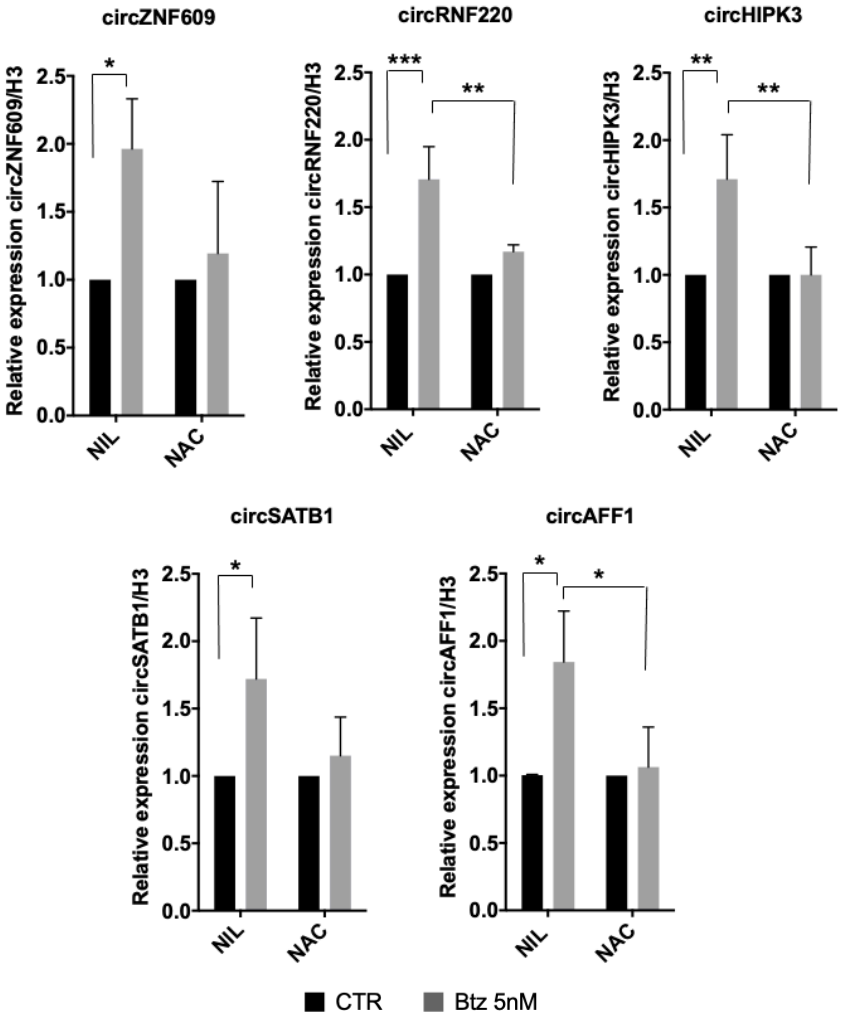

Figure 4.17. RT-qPCR analysis of circZNF609, circRNF220, circAFF1, circHIPK3 and circSATB1 in control and Btz-treated samples in MOLM13 treated with water (control) or with 5nM of Btz. N=3 *P≤0.05; **P≤0.005; ***P≤0.000; statistical analysis was performed by Two-Way ANOVA.

5. DISCUSSION

Acute myeloid leukemia is a blood disease in which hematopoietic progenitors are arrested at precise differentiation stages, becoming leukemic blasts characterized by uncontrolled proliferation rate. To date, the incidence of this malignancy is 4.3 per 100,000 annually in the United States (US), most common in adults (with ages > 68), but there are also cases in children[139]. The treatment most widely used is still chemotherapy, followed or not, by hematopoietic stem cells transplantation when possible, but this is not always the best strategy, especially in the elderly[140]. Most of these malignancies are characterized by chromosome inversions and translocations, or mutations, that result in the production of mutant or fusion proteins. Some of these cannot be properly folded causing accumulation of misfolded proteins in the ER and ER stress, subsequent activation of the UPR and stress resolution[141]. In general tumor cells are characterized by high levels of stress, due to mutations, hypoxic environment and oxidative stress. In order to resolve these kinds of stress, cancer cells adapt by upregulating pro-survival stress responses like the UPR and the oxidative stress response[142,143]. Several research groups have highlighted these aspects and how this balance can be disturbed by inducing death of cancer cells using cellular stress inducers, for example blocking protein glycosylation rather than the machinery responsible for protein degradation. Some AML subtypes, as described above, are characterized by fusion proteins, and some of these, like FLT3-ITD mutation, fail to be properly folded, causing an overload of misfolded proteins, which together with the physiological percentage of misfolded proteins create a variety of cellular stress. For these reasons the AML subtypes characterized by such proteins are much more sensitive to pharmacological induction of proteostatic stress compared to other tumors or to healthy cells. In recent years, many researchers have tried to use compounds that can induce stress and promote cell death alone or in combination with other drugs. Our lab set up a combination of drugs, tunicamycin, arsenic trioxide and retinoic

acid at physiological doses to induce ER stress and oxidative stress[144]. We used doses of each drug that were not able to induce cell death when used alone, but in combination led to 60-80% of leukemic cell death[145]. Another stress inducer is the proteosome inhibitor Bortezomib (Btz), the first one approved by the Food and Drug Administration. Btz is used for the treatment of mantle cell lymphoma and multiple myeloma, since it induces apoptosis of cancer cell, by binding the 26S proteasome[146].
Btz alone is capable of inducing strong cellular stress, in fact it induces ER stress, activates the oxidative stress response and autophagy.
Despite this, Btz, as single agent, is not used for the treatment of AML, which needs further investigation.
AML, in addition to fusion proteins, translocations and inversions, which cause tumor progression and drug resistance, are characterized by high expression of enzymes responsible for N6-methyladenosine or m^6A modification. m^6A is one of the most abundant, dynamic and reversible internal RNA modifications, which can be written by writer enzymes, removed by eraser enzymes and read by specific and numerous reader enzymes[147]. METTL3, the main player of this RNA modification, is highly expressed in AML, along with METTL14, the cofactor WTAP, and the erasers FTO and ALKBH5. Their deregulation is implicated in uncontrolled proliferation of leukemic stem cells through the induction of oncogenes and anti-apoptotic pathways[148]. In recent years, the role of m^6A has also been highlighted in the biogenesis and translation of a new class of ncRNAs, the circRNAs. CircRNAs are generated by a peculiar kind of splicing, known as back-splicing, in which the 5' end binds the 3' end upstream, generating a covalently closed circular structure. The presence of the m^6A modification on the transcript promotes one splicing rather than another, thus generating circRNAs[149]. Furthermore, it is now known that due to the presence of this RNA modification, some circRNAs can be translated into peptides[75,76].

Both, m^6A and circRNAs are involved in stress induction and response, but this field is still unclear and deserves elucidation. Based on what has been described so far, and as the role of Btz on m^6A and circRNAs is unknown, we wondered whether modulation of m^6A-modified circRNAs could contribute to induce or protect against the Btz-induced stress response.

To answer this question, we decided to treat MOLM13 cell line with the proteasome inhibitor, Btz, to induce acute stress and see what the effect on m^6A enzyme expression was. Surprisingly, we observed a downregulation of protein expression levels (but not of the messenger RNAs) of some m^6A enzymes. Our focus was on WTAP, which protein expression levels decreased strongly after Btz treatment. WTAP was one of the first m^6A cofactors to be discovered and correlated with this modification[93]. Its deregulation in AML is known and demonstrated by numerous groups[96,150]. What was certainly not known is its short half-life, as demonstrated in this work. Given the sharp and drastic drop in protein expression levels of WTAP upon Btz treatment, we wondered if this was due to its weak stability. We found that WTAP has a very short half-life and this could explain the strong reduction of protein expression levels, already after 16h of treatment with the lowest dose of Btz.

The stress response is a finely regulated response and different concentrations and/or conditions can lead to different effects. The Btz concentrations that we used in AML cell line, induced ISR activation, as evidenced by phosphorylation of eIF2α and the resulting reduction in overall protein synthesis.

Inhibition of protein synthesis is a response that cells put in place in an attempt to resolve impending stress by alleviating cellular damage, or alternatively, by inducing apoptosis. This conserves energy and promotes the translation of stress-specific mRNAs, such as ATF4[151]. The preferential translation of ATF4 under stress conditions, is due to the presence of two upstream ORFs (uORFs), the second of which is inhibitory; high expression of P-eIF2α with inhibition of synthesis, leads to bypass this second inhibitory uORF and to translate ATF4[152]. However, in recent work it was observed

that ATF4 mRNA shows methylation zones, some of which are within uORF2, and that these methylation levels drop under starvation conditions so also this modification could play a role in ATF4 regulation[153].
Btz treatment also generated oxidative stress, which we conclude that contributes to the lowered protein expression levels of WTAP, as evidenced by its recovery following NAC administration. NAC is one of the most used antioxidants to prevent or alleviate the effects of oxidative stress, since it is a precursor for glutathione biosynthesis, reduces disulphide bonds and acts as a scavenger of ROS[154].
Certainly, in an antioxidant environment, the cell is able to perform all its functions, including protein folding, translation, and stress response in general, at the best of its ability. The activation of Hmox, a target gene of the oxidative stress response, confirm the attempt to recover homeostasis.
In our work we have shown that stress, mostly oxidative stress, has a negative influence on overall m^6A levels. Since m^6A also regulates the biogenesis of circRNAs and their translation in some cases, it was of crucial importance to investigate possible m^6A-modified circRNAs that might play a role in the Btz-induced stress response. In particular, blocking of general translation could induce the preferential translation of certain circRNAs presenting the m^6A RNA modification and therefore these could be more highly expressed under stress conditions, in the same way as ATF4. Surprisingly, m^6A-IP followed by circ-sequencing, showed that, despite the general decrease in m^6A RNA methylation, there were 47 hyper-methylated and 8 hypo-methylated circRNAs upon Btz treatment, compared to control samples. We decided to analyze five of these hyper-methylated circRNAs, those that were most enriched in the samples immunoprecipitated for m^6A. Of particular interest is circRNF220, which has been shown to be over-expressed in AML and associated with relapse in pediatric acute myeloid leukemia[155]. CircZNF609, which can be translated both by IRES-driven pathway[75], but also thanks to the m^6A modification through

recognition by YTHDF3 and eIF4G2[65].CcircZNF609, is highly expressed in endothelial cells, myoblasts and neuroses, but also in numerous tumors. Interestingly, two different research groups have highlighted its protective role against oxidative and hypoxia stress in both endothelial cells and retinal neurodegeneration[156,157]. Similarly, circHIPK3 plays a role in the regulation of autophagy and apoptosis in several malignancies[158]. Furthermore, elevated expression of circHIPK3 was observed in hypoxic exosomes, compared to normoxic exosomes. The presence of circHIPK3 in the exosomes plays an important role in alleviating the oxidative stress induced by cardiac myxovascular endothelial cells dysfunction[159]. Regarding circAFF1 and circSATB1, their role is still poorly understood, especially in cellular stress conditions.

One of the problems most frequently encountered in the treatment of AML are relapses and/or resistance to certain drugs or inhibitors. In the clinic, there are numerous drugs approved for the treatment of AML which inhibit specific molecular targets involved in tumorigenesis. One of these is Venetoclax, specific inhibitor of B cell lymphoma 2 (BCL-2), which as single agents or in combination with hypomethylating agents, such as azacitidine, is now approved as first-line therapy among elderly and patients with newly diagnosed AML ineligible for standard chemotherapy[160]. However, many patients acquire resistance after both single and combination treatment. The use of FLT3 inhibitors for the treatment of FLT3-ITD mutated AML is also approved, but relapse still remains the main cause of therapeutic failure. Studies of possible combinations between Venetoclax and FLT3 inhibitors are currently ongoing, as FLT3 mutations are among the most common mechanisms contributing to Venetoclax resistance[161,162].

For these reasons, it is important to look for new combinations and to study resistance markers using resistant cell lines or primary cells. To this end, we decided to create Btz-resistant lines by exposing the cells to treatment with increasing doses of the proteosome inhibitor, Btz.

Btz-resistant cells not only didn't undergo cell death after 72 hours of treatment at the same conditions that induce 100% of cell death in the parental cell line (MOLM13), but also showed no changes in m^6A protein expression levels compared to MOLM13 cell line treated with Btz. Furthermore, the same circRNAs that were up-regulated in MOLM13 cell line upon treatment with Btz, showed no increased expression in Btz-resistant clone 3 undergoing the same treatment. At the same way, MOLM13 cell line treated with Btz after pre-treatment with NAC, showed no increase of the same circRNAs, indicating their possible role in mediating the oxidative stress response. Nevertheless, further investigations are still needed to elucidate the full picture of this complex OxS-m^6A-circRNAs axis induced by Btz in AML progression and resistance.
In conclusion my work demonstrated that proteotoxic stress induced by proteasome inhibition affects m^6A modification pathways and the methylation and expression of specific circRNAs that could be important molecular target to understand AML resistance to treatments (the disserted mechanism is represented in the Figure 5.1).

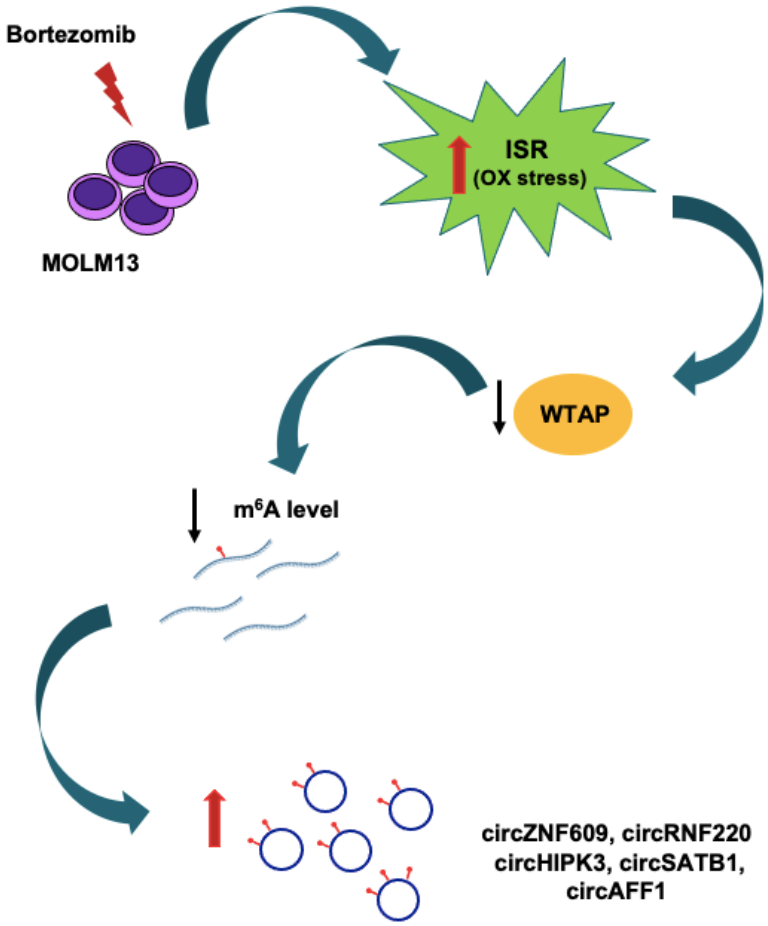

Figure 5.1. Btz treatment, in AML cells, activates the ISR and oxidative stress, which downregulate m^6A enzymes, in particular WTAP, and m^6A modification levels. Nevertheless, some circRNAs are hypermethylated and upregulated upon Btz treatment and they could have an important role in regulating Btz-mediated stress response.

6. MATERIALS AND METHODS

6.1 Cell culture and treatments

MOLM-13 cell lines were cultured with RPMI 1640 (Gibco® Thermo Fisher Scientific, Waltham, MA USA) enriched with pen/strep (50 U/mL) and with 10% heat-inactivated South-American Fetal Bovine Serum (FBS) (Gibco® Thermo Fisher Scientific), at 37°C and 5% CO2.
MOLM-13 cells were treated with 5nM Bortezomib (Btz, Sigma-Aldrich) and 10nM Btz at 6h, 16h and 24h. About the treatment with N-acetylcysteine (NAC, Sigma-Aldrich), cells were pre-treated with NIL (control sample with sterilized water) and with NAC and the day after with Btz.
MOLM-13 cell line resistant to Btz was established through exposing MOLM-13 cells to continuous presence of stepwise escalating levels of Btz. After 4 months, clones were selected, and the experiments were performed as previously described.
MOLM-13 cells were treated with puromycin (#ant-pr-1, InvivoGen) at 10ug/ml after 16h of Btz treatment. Incorporated puromycin protein level was then analyzed 0, 10 and 30 minutes after treatment by Western Blot analysis. For protein stability assay, cells were treated with 10ug/mL cycloheximide (CHX, Sigma-Aldrich) for 1 and 3h.

6.2 RNA extraction and real-time qRT-PCR analysis

Total RNA was extracted using the TRIzol RNA Isolation System (Invitrogen) according to manufacturer instructions. Reverse transcription to cDNA was performed with the High-Capacity RNA-to-cDNA Kit (Applied Biosystems) and cDNA was amplified using the SYBR™ Green PCR Master Mix and TaqMan Universal PCR Master Mix (Thermo Fisher Scientific) on an ABI PRISM 7500 Sequence Detection System (Applied Biosystems). The following oligo sequences were used:

Target		Sequence oligo
WTAP	SYBR	For 5'-GGCGAAGTGTCGAATGCT-3' Rev 5'-CCAACTGCTGGCGTGTCT-3'
METTL3	SYBR	For 5'-AAGCAGCTGGACTCTCTGCG-3' Rev 5'-GCACTGGGCTGTCACTACGG-3'
FTO	SYBR	For 5'-TGGGTTCATCCTACAACGG-3' Rev 5'-CCTCTTCAGGGCCTTCAC-3
YTHDF2	SYBR	For 5'-GAACCTTACTTGAGTCCACAG-3' Rev 5'-GTAGGGCATGGCTGTGTCAC-3'
YTHDC1	SYBR	For 5'--3' Rev 5'-3'
circZNF609	SYBR	For 5'-AAACCGGAGCCAGAGGAAGG-3' Rev 5'-CAGCTATGTTCTCAGACCTGC-3'
circRNF220	SYBR	For 5'-TCTGATCGGGAAGCCTCATC-3' Rev 5'-TCGGAGTCTCTTTCTGTGGC-3'
circHIPK3	SYBR	For 5'-CGGCCAGTCATGTATCAAAGA-3' Rev 5'-ACAACTGCTTGGCTCTACTTTG-3'
circSATB1	SYBR	For 5'-CGTGCTAAAGTGTCTCAAGC-3' Rev 5'-GACCCTTCGGATCACTCACA-3'

circAFF1	SYBR	For 5'-CCTGAACTGAAACCACTGCC-3' Rev 5'- CCTGGTTGCGTCTTTCCTTC -3'
H3	SYBR	For 5'-GTGAAGAAACCTCATCGTTACAGGC CTGGT -3' Rev 5'-CTGCAAAGCACCAATAGCTGCACTC TGGAA -3'
GAPDH	TaqMan	Primer 1 5'-ACATCGCTCAGACACCATG-3' Primer 2 5'-TGTAGTTGAGGTCAATGAAGGG-3'
Hmox	TaqMan	Primer 1 5'-TCATGAGGAACTTTCAGAAGGG-3' Primer 2 5'-TGCGCTCAATCTCCTCCT-3'

6.3 Lysis and immunoblotting analysis

Cells were lysed RIPA buffer and fresh protease inhibitors. Cells were sonicated 10 seconds and centrifuged for 10 minutes at 12000 x rpm. Lysates were quantified using Bradford Assay Reagent (#1863028, Thermo Fisher, USA). Protein samples were separated by SDS-PAGE and transferred onto a nitrocellulose membrane. The membrane was incubated overnight with the following primary antibodies: rabbit monoclonal anti-METTL3 (#ab195352, Abcam); mouse monoclonal anti-WTAP (#60188-1-Ig, Proteintech); rabbit polyclonal anti-FTO (#27226-1-AP, Proteintech); rabbit polyclonal anti-YTHDF2 (#ARP67917_P050, Aviva); rabbit polyclonal anti-YTHDC1 (#ab122340, Abcam); mouse monoclonal anti-BiP/GRP78 (#610978, BD); rabbit monoclonal anti-Phospho-eIF2α (Ser51) (#D9G8, Cell Signaling); rabbit monoclonal anti-H3 (#ab1791, Abcam); mouse monoclonal anti-Puromycin, clone

12D10 (#MABE343, Millipore); mouse monoclonal anti-GAPDH 6C5 (#sc32233, Santa Cruz Biotechnology); mouse monoclonal anti-Tubulin B512 (#T5168, Sigma-Aldrich). For the detection we used ECL method (Enhanced ChemiLuminescence) (Amersham Biosciences) using ChemiDoc-It Imaging System (UVP, Upland, CA) instrument.

6.4 Immunofluorescence

10^6 CTR and Btz treated cells were collected and stained with Cytofix/Cytoperm Fixation/Permeabilization solution Kit (#BD554714, Becton Dickinson) according to the manufacturer's instructions. Cells were fixed in Fix Perm for 20 minutes at 4°C, rinsed with Wash Perm and incubated with the primary antibody anti-m^6A. After two Wash Perm washes, cells were incubated with the secondary antibody Alexa Fluor 488-labeled goat anti-rabbit (#A-11034, Invitrogen). The nuclei were stained with Hoechst 33342 (Life Technologies) for 5 min in Wash Perm. Cells were rinsed, seeded on the slides (200000 cells) and mounted in VECTASHIELD antifade mounting media (#H-1000, Vector Laboratories). Images were acquired using a Zeiss LSM 900 confocal laser scanning microscope.

6.5 ROS Detection.

ROS levels were measure via oxidation-sensitive 2', 7'-dichlorodihydrofluorescein diacetate (H2DCFDA)-mediated fluorescence, according to the manufacturer's protocol.

6.6 m^6A immunoprecipitation

Cells were treated with 5nM of Btz and after 16h total RNA was extracted. The samples were treated with RNAseR, in order to remove all the linear RNA. A fraction of the RNA was collected as input sample and the rest was incubated with m^6A-specific antibody (#ab151230, Abcam) or with control rabbit IgG (Millipore) antibody for 2h at 4 °C on rotator. Immunoprecipitated RNA was eluted and resuspended in RNase-free water. Same procedure, but without

RNAse R treatment was performed on new biological replicates, to validate the RNAseq data.

6.7 CircRNAs Sequencing

The purified RNA was quantified with by NanoDrop. The size distribution of the RNA was controlled on a Bioanalyzer with the Agilent RNA 6000 Pico Kit (Agilent Technologies, Santa Clara, CA, USA). The RNA libraries for sequencing were prepared with the SMARTer Stranded Total RNA Sample Prep Kit - Low Input Mammalian (Takara Bio. USA, Inc). The quality of the final libraries was controlled on a Bioanalyzer using the High Sensitivity DNA Kit (Agilent Technologies, Santa Clara, CA, USA). The quantification of the libraries was performed by qPCR. Sequencing was carried out on a NovaSeq 6000 instrument (Illumina Inc., San Diego, CA, USA), sequencing in paired-end mode 101bp.

6.8 Computational Analysis of circRNA-seq

Quality of RNA-seq was evaluated through FASTQC tool v0.11.9 (http://www.bioinformatics.babraham.ac.uk/projects/fastqc/) for each sample and combined with multiqc tool v.1.9[163]. The length of RNA-seq fragments was checked to ensure the efficiency of further fragments alignment. After that, back spliced junctions (BSJ) were detected and aligned to the reference genome (hg19) by using STAR v2.7.9a[164] (parameters for BSJ: --chimJunctionOverhangMin 15, --chimOutType Junctions SeparateSAMold, -- chimScoreMin 15, --chimScoreSeparation 10, --chimSegmentMin 10). The tool returned also a separate file with information related to aligned reads that are not BSJ. The sorted alignments were indexed by using the index function of samtools v1.9. The parse module of CIRCExplorer2 v.2.3.8 software[165] (parameter: -t STAR) was used to extract the coordinates of fragments mapping to BSJ sites. These were annotated through the annotate module of CIRCExplorer2 which used already known GENECODE annotation of hg19. The quantification of detected circRNA was executed with CIRIquant toolkit[166] v.1.1.2. The inputs for this process were the fastq files and

the coordinates of BSJ sites. Two independent matrices were generated with the circRNA and gene expression data by respectively utilizing prep_CIRIquant and prepDE.py tools of CIRIquant. The differential expression (DE) analysis was implemented through CIRI_DE_replicate tool of CIRIquant. The DE results were shown in a volcano plot carried out with the ggplot package in R. Principal component analysis (PCA) was executed pre- and postnormalization. PCA was executed using the function prcomp of stats v.4.0.2 R package and plotted through the function autoplot of ggfortify v.0.4.11 R package.

6.9 Statistical analysis

The statistical analyses were performed using GraphPad Prism (GraphPad Software, San Diego, California, USA). Statistical analysis to determine significance was performed using Student's *t* tests or One-Way Anova test. Differences were considered statistically significant at the $p < 0.05$ level.

BIBLIOGRAPHY

1. Desrosiers, R., Friderici, K. & Rottman, F. Identification of Methylated Nucleosides in Messenger RNA from Novikoff Hepatoma Cells. *Proc. Natl. Acad. Sci. U. S. A.* **71**, 3971 (1974).
2. Bokar, J. A., Shambaugh, M. E., Polayes, D., Matera, A. G. & Rottman, F. M. Purification and cDNA cloning of the AdoMet-binding subunit of the human mRNA (N6-adenosine)-methyltransferase. *RNA* **3**, 1233–1247 (1997).
3. Dominissini, D. *et al.* Topology of the human and mouse m6A RNA methylomes revealed by m6A-seq. *Nature* **485**, 201–206 (2012).
4. Cron, M. A., Guillochon, É., Kusner, L. & Le Panse, R. Role of miRNAs in Normal and Myasthenia Gravis Thymus. *Front. Immunol.* **11**, 1074 (2020).
5. Csepanys, T., Lint, A., Baldick, C. J. & Beemonq, K. Sequence specificity of mRNA N6-adenosine methyltransferase. *J. Biol. Chem.* **265**, 20117–20122 (1990).
6. Śledź, P. & Jinek, M. Structural insights into the molecular mechanism of the m6A writer complex. *Elife* **5**, e18434 (2016).
7. Lesbirel, S. & Wilson, S. A. The m6A-methylase complex and mRNA export. *Biochim. Biophys. Acta. Gene Regul. Mech.* **1862**, 319 (2019).
8. Ping, X. L. *et al.* Mammalian WTAP is a regulatory subunit of the RNA N6-methyladenosine methyltransferase. *Cell Res.* **24**, 177–189 (2014).
9. Liu, J. *et al.* VIRMA mediates preferential m6A mRNA methylation in 3′UTR and near stop codon and associates with alternative polyadenylation. *Cell Discov.* **4**, (2018).
10. Wen, J. *et al.* Zc3h13 regulates nuclear RNA m6A methylation and mouse embryonic stem cell self-renewal.

Mol. Cell **69**, 1028 (2018).
11. Knuckles, P. *et al.* Zc3h13/Flacc is required for adenosine methylation by bridging the mRNA-binding factor Rbm15/Spenito to the m 6 A machinery component Wtap/Fl(2)d. *Genes Dev.* **32**, 415–429 (2018).
12. Doxtader, K. A. *et al.* Structural Basis for Regulation of METTL16, an S-Adenosylmethionine Homeostasis Factor. *Mol. Cell* **71**, 1001-1011.e4 (2018).
13. Satterwhite, E. R. & Mansfield, K. D. RNA methyltransferase METTL16: Targets and function. *Wiley Interdiscip. Rev. RNA* **13**, (2022).
14. Pinto, R. *et al.* The human methyltransferase ZCCHC4 catalyses N6-methyladenosine modification of 28S ribosomal RNA. *Nucleic Acids Res.* **48**, 830–846 (2020).
15. Van Tran, N. *et al.* The human 18S rRNA m6A methyltransferase METTL5 is stabilized by TRMT112. *Nucleic Acids Res.* **47**, 7719–7733 (2019).
16. Jia, G. *et al.* N6-Methyladenosine in nuclear RNA is a major substrate of the obesity-associated FTO. *Nat. Chem. Biol.* **7**, 885–887 (2011).
17. Zheng, G. *et al.* ALKBH5 Is a Mammalian RNA Demethylase that Impacts RNA Metabolism and Mouse Fertility. *Mol. Cell* **49**, 18–29 (2013).
18. Wang, X. *et al.* N6-methyladenosine modulates messenger RNA translation efficiency. *Cell* **161**, 1388–1399 (2015).
19. Mauer, J. *et al.* Reversible methylation of m 6 A m in the 5' cap controls mRNA stability. *Nature* **541**, 371–375 (2017).
20. Xu, C. *et al.* Structures of human ALKBH5 demethylase reveal a unique binding mode for specific single-stranded N6-methyladenosine RNA demethylation. *J. Biol. Chem.* **289**, 17299–17311 (2014).
21. Roost, C. *et al.* Structure and thermodynamics of N6-methyladenosine in RNA: a spring-loaded base modification. *J. Am. Chem. Soc.* **137**, 2107–2115 (2015).
22. Rajagopalan, L. E., Westmark, C. J., Jarzembowski, J. A. &

Malter, J. S. hnRNP C increases amyloid precursor protein (APP) production by stabilizing APP mRNA. *Nucleic Acids Res.* **26**, 3418–3423 (1998).
23. Zarnack, K. *et al.* Direct competition between hnRNP C and U2AF65 protects the transcriptome from the exonization of Alu elements. *Cell* **152**, 453–466 (2013).
24. McCloskey, A., Taniguchi, I., Shinmyozu, K. & Ohno, M. hnRNP C tetramer measures RNA length to classify RNA polymerase II transcripts for export. *Science* **335**, 1643–1646 (2012).
25. Liu, N. *et al.* N6 -methyladenosine-dependent RNA structural switches regulate RNA-protein interactions. *Nature* **518**, 560–564 (2015).
26. Liu, N. *et al.* N6-methyladenosine alters RNA structure to regulate binding of a low-complexity protein. *Nucleic Acids Res.* **45**, 6051–6063 (2017).
27. Alarcón, C. R. *et al.* HNRNPA2B1 is a mediator of m6A-dependent nuclear RNA processing events. *Cell* **162**, 1299 (2015).
28. Zhou, K. I., Shi, H., He, C. & Parisien, M. Regulation of Co-transcriptional Pre-mRNA Splicing by m 6 A through the Low-Complexity Protein hnRNPG. *Mol. Cell* **76**, 70-81.e9 (2019).
29. Liao, S., Sun, H. & Xu, C. YTH Domain: A Family of N6-methyladenosine (m6A) Readers. *Genomics. Proteomics Bioinformatics* **16**, 99–107 (2018).
30. Sun, J., Bie, X. M., Wang, N., Zhang, X. S. & Gao, X. Q. Genome-wide identification and expression analysis of YTH domain-containing RNA-binding protein family in common wheat. *BMC Plant Biol.* **20**, (2020).
31. Li, F., Zhao, D., Wu, J. & Shi, Y. Structure of the YTH domain of human YTHDF2 in complex with an m6A mononucleotide reveals an aromatic cage for m6A recognition. *Cell Res. 2014 2412* **24**, 1490–1492 (2014).
32. Luo, S. & Tong, L. Molecular basis for the recognition of

methylated adenines in RNA by the eukaryotic YTH domain. *Proc. Natl. Acad. Sci. U. S. A.* **111**, 13834–13839 (2014).
33. Kasowitz, S. D. *et al.* Nuclear m6A reader YTHDC1 regulates alternative polyadenylation and splicing during mouse oocyte development. *PLoS Genet.* **14**, (2018).
34. Roundtree, I. A. *et al.* YTHDC1 mediates nuclear export of N6-methyladenosine methylated mRNAs. *Elife* **6**, e31311 (2017).
35. Li, L. *et al.* The XRN1-regulated RNA helicase activity of YTHDC2 ensures mouse fertility independently of m6A recognition. *Mol. Cell* **82**, 1678-1690.e12 (2022).
36. Wojtas, M. N. *et al.* Regulation of m 6 A Transcripts by the 3′→5′ RNA Helicase YTHDC2 Is Essential for a Successful Meiotic Program in the Mammalian Germline. *Mol. Cell* **68**, 374-387.e12 (2017).
37. Hsu, P. J. *et al.* Ythdc2 is an N6 -methyladenosine binding protein that regulates mammalian spermatogenesis. *Cell Res.* **27**, 1115–1127 (2017).
38. Ivanova, I. *et al.* The RNA m6A Reader YTHDF2 Is Essential for the Post-transcriptional Regulation of the Maternal Transcriptome and Oocyte Competence. *Mol. Cell* **67**, 1059-1067.e4 (2017).
39. Wang, X. *et al.* N 6-methyladenosine-dependent regulation of messenger RNA stability. *Nature* **505**, 117–120 (2014).
40. Du, H. *et al.* YTHDF2 destabilizes m(6)A-containing RNA through direct recruitment of the CCR4-NOT deadenylase complex. *Nat. Commun.* **7**, (2016).
41. Shi, H. *et al.* YTHDF3 facilitates translation and decay of N 6-methyladenosine-modified RNA. *Cell Res.* **27**, 315–328 (2017).
42. Fustin, J. M. *et al.* XRNA-methylation-dependent RNA processing controls the speed of the circadian clock. *Cell* **155**, 793 (2013).
43. Li, H. *et al.* METTL3 promotes cell cycle progression via m

6 A/YTHDF1-dependent regulation of CDC25B translation. *Int. J. Biol. Sci.* **18**, 3223–3236 (2022).
44. Zhao, X. *et al.* FTO-dependent demethylation of N6-methyladenosine regulates mRNA splicing and is required for adipogenesis. *Cell Res.* **24**, 1403–1419 (2014).
45. Zhang, C. *et al.* m 6 A modulates haematopoietic stem and progenitor cell specification. *Nature* **549**, 273–276 (2017).
46. Lee, H. *et al.* Stage-specific requirement for Mettl3-dependent m 6 A mRNA methylation during haematopoietic stem cell differentiation. *Nat. Cell Biol.* **21**, 700–709 (2019).
47. Yao, Q. J. *et al.* Mettl3-Mettl14 methyltransferase complex regulates the quiescence of adult hematopoietic stem cells. *Cell Res.* **28**, 952–954 (2018).
48. Sanger, H. L., Klotz, G., Riesner, D., Gross, H. J. & Kleinschmidt, A. K. Viroids are single-stranded covalently closed circular RNA molecules existing as highly base-paired rod-like structures. *Proc. Natl. Acad. Sci. U. S. A.* **73**, 3852–3856 (1976).
49. Hsu, M. T. & Coca-Prados, M. Electron microscopic evidence for the circular form of RNA in the cytoplasm of eukaryotic cells. *Nat. 1979 2805720* **280**, 339–340 (1979).
50. Cocquerelle, C., Daubersies, P., Majerus, M. A., Kerckaert, J. P. & Bailleul, B. Splicing with inverted order of exons occurs proximal to large introns. *EMBO J.* **11**, 1095–1098 (1992).
51. C, C., B, M., D, H. & B, B. Mis-splicing yields circular RNA molecules. *FASEB J.* **7**, 155–160 (1993).
52. Gao, Y., Wang, J. & Zhao, F. CIRI: An efficient and unbiased algorithm for de novo circular RNA identification. *Genome Biol.* **16**, 1–16 (2015).
53. Meganck, R. M. *et al.* Tissue-Dependent Expression and Translation of Circular RNAs with Recombinant AAV Vectors In Vivo. *Mol. Ther. Nucleic Acids* **13**, 89–98 (2018).
54. Rybak-Wolf, A. *et al.* Circular RNAs in the Mammalian

Brain Are Highly Abundant, Conserved, and Dynamically Expressed. *Mol. Cell* **58**, 870–885 (2015).
55. Gao, Y. *et al.* Comprehensive identification of internal structure and alternative splicing events in circular RNAs. *Nat. Commun. 2016 71* **7**, 1–13 (2016).
56. Chen, L. *et al.* The bioinformatics toolbox for circRNA discovery and analysis. *Brief. Bioinform.* **22**, 1706–1728 (2021).
57. Chen, L. L. The expanding regulatory mechanisms and cellular functions of circular RNAs. *Nat. Rev. Mol. Cell Biol. 2020 218* **21**, 475–490 (2020).
58. Kelly, S., Greenman, C., Cook, P. R. & Papantonis, A. Exon Skipping Is Correlated with Exon Circularization. *J. Mol. Biol.* **427**, 2414–2417 (2015).
59. Ashwal-Fluss, R. *et al.* circRNA biogenesis competes with pre-mRNA splicing. *Mol. Cell* **56**, 55–66 (2014).
60. Jeck, W. R. *et al.* Circular RNAs are abundant, conserved, and associated with ALU repeats. *RNA* **19**, 141–157 (2013).
61. Errichelli, L. *et al.* FUS affects circular RNA expression in murine embryonic stem cell-derived motor neurons. *Nat. Commun. 2017 81* **8**, 1–11 (2017).
62. Conn, S. J. *et al.* The RNA Binding Protein Quaking Regulates Formation of circRNAs. *Cell* **160**, 1125–1134 (2015).
63. Conn, S. J. *et al.* The RNA binding protein quaking regulates formation of circRNAs. *Cell* **160**, 1125–1134 (2015).
64. Yuan, Y. *et al.* Muscleblind-like 1 interacts with RNA hairpins in splicing target and pathogenic RNAs. *Nucleic Acids Res.* **35**, 5474 (2007).
65. Di Timoteo, G. *et al.* Modulation of circRNA Metabolism by m6A Modification. *Cell Rep.* (2020). doi:10.1016/j.celrep.2020.107641
66. Li, X., Yang, L. & Chen, L. L. The Biogenesis, Functions, and Challenges of Circular RNAs. *Mol. Cell* **71**, 428–442

(2018).
67. Li, Z., Kearse, M. G. & Huang, C. The nuclear export of circular RNAs is primarily defined by their length. *RNA Biol.* **16**, 1 (2019).
68. Li, Z. *et al.* Exon-intron circular RNAs regulate transcription in the nucleus. *Nat. Struct. Mol. Biol. 2015 223* **22**, 256–264 (2015).
69. Holdt, L. M., Kohlmaier, A. & Teupser, D. Molecular roles and function of circular RNAs in eukaryotic cells. *Cell. Mol. Life Sci.* **75**, 1071 (2018).
70. Memczak, S. *et al.* Circular RNAs are a large class of animal RNAs with regulatory potency. *Nature* **495**, 333–338 (2013).
71. Jiang, C. *et al.* The Emerging Picture of the Roles of CircRNA-CDR1as in Cancer. *Front. Cell Dev. Biol.* **8**, 590478 (2020).
72. Hansen, T. B. *et al.* miRNA-dependent gene silencing involving Ago2-mediated cleavage of a circular antisense RNA. *EMBO J.* **30**, 4414–4422 (2011).
73. Ng, W. L. *et al.* Inducible RasGEF1B circular RNA is a positive regulator of ICAM-1 in the TLR4/LPS pathway. *RNA Biol.* **13**, 861 (2016).
74. Du, W. W. *et al.* Foxo3 circular RNA retards cell cycle progression via forming ternary complexes with p21 and CDK2. *Nucleic Acids Res.* **44**, 2846 (2016).
75. Legnini, I. *et al.* Circ-ZNF609 Is a Circular RNA that Can Be Translated and Functions in Myogenesis. *Mol. Cell* **66**, 22-37.e9 (2017).
76. Yang, Y. *et al.* Extensive translation of circular RNAs driven by N 6-methyladenosine. *Cell Res.* **27**, 626–641 (2017).
77. Liccardo, F., Iaiza, A., Śniegocka, M., Masciarelli, S. & Fazi, F. Circular RNAs Activity in the Leukemic Bone Marrow Microenvironment. *Non-coding RNA* **8**, 50 (2022).
78. Meng, S. *et al.* CircRNA: functions and properties of a

novel potential biomarker for cancer. *Mol. Cancer* **16**, (2017).
79. Showel, M. M. & Levis, M. Advances in treating acute myeloid leukemia. *F1000Prime Rep.* **6**, (2014).
80. Thein, M. S., Ershler, W. B., Jemal, A., Yates, J. W. & Baer, M. R. Outcome of older patients with acute myeloid leukemia: an analysis of SEER data over 3 decades. *Cancer* **119**, 2720–2727 (2013).
81. Dores, G. M., Devesa, S. S., Curtis, R. E., Linet, M. S. & Morton, L. M. Acute leukemia incidence and patient survival among children and adults in the United States, 2001-2007. *Blood* **119**, 34–43 (2012).
82. Bennett, J. M. *et al.* Proposals for the classification of the acute leukaemias. French-American-British (FAB) co-operative group. *Br. J. Haematol.* **33**, 451–458 (1976).
83. Vardiman, J. W. *et al.* The 2008 revision of the World Health Organization (WHO) classification of myeloid neoplasms and acute leukemia: rationale and important changes. *Blood* **114**, 937–951 (2009).
84. Arber, D. A. *et al.* The 2016 revision to the World Health Organization classification of myeloid neoplasms and acute leukemia. *Blood* **127**, 2391–2405 (2016).
85. Khoury, J. D. *et al.* The 5th edition of the World Health Organization Classification of Haematolymphoid Tumours: Myeloid and Histiocytic/Dendritic Neoplasms. *Leuk. 2022 367* **36**, 1703–1719 (2022).
86. Levis, M. *et al.* Internal tandem duplications of the FLT3 gene are present in leukemia stem cells. *Blood* **106**, 673 (2005).
87. Takahashi, S. Mutations of FLT3 receptor affect its surface glycosylation, intracellular localization, and downstream signaling. *Leuk. Res. Reports* **13**, 100187 (2020).
88. Liquori, A. *et al.* Acute Promyelocytic Leukemia: A Constellation of Molecular Events around a Single PML-RARA Fusion Gene. *Cancers (Basel).* **12**, (2020).

89. Meyer, C. *et al.* The MLL recombinome of acute leukemias. *Leukemia* **20**, 777–784 (2006).
90. McCulloch, D., Brown, C. & Iland, H. Retinoic acid and arsenic trioxide in the treatment of acute promyelocytic leukemia: current perspectives. *Onco. Targets. Ther.* **10**, 1585 (2017).
91. Dombret, H. & Gardin, C. An update of current treatments for adult acute myeloid leukemia. *Blood* **127**, 53 (2016).
92. Kantarjian, H. *et al.* Acute myeloid leukemia: current progress and future directions. *Blood Cancer J. 2021 112* **11**, 1–25 (2021).
93. Little, N. A., Hastie, N. D. & Davies, R. C. Identification of WTAP, a novel Wilms' tumour 1-associating protein. *Hum. Mol. Genet.* **9**, 2231–2239 (2000).
94. Yang, L., Han, Y., Saurez Saiz, F. & Minden, M. D. A tumor suppressor and oncogene: the WT1 story. *Leuk. 2007 215* **21**, 868–876 (2007).
95. Bansal, H. *et al.* WTAP is a novel oncogenic protein in acute myeloid leukemia. *Leuk. 2014 285* **28**, 1171–1174 (2014).
96. Naren, D. *et al.* High Wilms' tumor 1 associating protein expression predicts poor prognosis in acute myeloid leukemia and regulates m 6 A methylation of MYC mRNA. *J. Cancer Res. Clin. Oncol.* **147**, 33–47 (2021).
97. Barbieri, I. *et al.* Promoter-bound METTL3 maintains myeloid leukaemia by m6A-dependent translation control. *Nature* **552**, 126–131 (2017).
98. Weng, H. *et al.* METTL14 Inhibits Hematopoietic Stem/Progenitor Differentiation and Promotes Leukemogenesis via mRNA m6A Modification. *Cell Stem Cell* **22**, 191-205.e9 (2018).
99. Cai, X. *et al.* HBXIP-elevated methyltransferase METTL3 promotes the progression of breast cancer via inhibiting tumor suppressor let-7g. *Cancer Lett.* **415**, 11–19 (2018).
100. Sorci, M. *et al.* METTL3 regulates WTAP protein

homeostasis. *Cell Death Dis.* (2018). doi:10.1038/s41419-018-0843-z
101. Li, Z. *et al.* FTO plays an oncogenic role in acute myeloid leukemia as a N6-methyladenosine RNA demethylase. *Cancer Cell* **31**, 127 (2017).
102. Shen, C. *et al.* RNA Demethylase ALKBH5 Selectively Promotes Tumorigenesis and Cancer Stem Cell Self-Renewal in Acute Myeloid Leukemia. *Cell Stem Cell* **27**, 64-80.e9 (2020).
103. Wang, J. *et al.* Leukemogenic Chromatin Alterations Promote AML Leukemia Stem Cells via a KDM4C-ALKBH5-AXL Signaling Axis. *Cell Stem Cell* **27**, 81-97.e8 (2020).
104. Paris, J. *et al.* Targeting the RNA m 6 A Reader YTHDF2 Selectively Compromises Cancer Stem Cells in Acute Myeloid Leukemia. *Cell Stem Cell* **25**, 137-148.e6 (2019).
105. Sheng, Y. *et al.* A critical role of nuclear m6A reader YTHDC1 in leukemogenesis by regulating MCM complex–mediated DNA replication. *Blood* **138**, 2838–2852 (2021).
106. Elcheva, I. A. *et al.* RNA-binding protein IGF2BP1 maintains leukemia stem cell properties by regulating HOXB4, MYB, and ALDH1A1. *Leukemia* **34**, 1354 (2020).
107. Han, F. *et al.* hsa_circ_0001947 suppresses acute myeloid leukemia progression via targeting hsa-miR-329-5p/CREBRF axis. *https://doi.org/10.2217/epi-2019-0352* **12**, 935–953 (2020).
108. Sun, Y. M. *et al.* CircMYBL2, a circRNA from MYBL2, regulates FLT3 translation by recruiting PTBP1 to promote FLT3-ITD AML progression. *Blood* **134**, 1533–1546 (2019).
109. Guarnerio, J. *et al.* Oncogenic Role of Fusion-circRNAs Derived from Cancer-Associated Chromosomal Translocations. *Cell* **165**, 289–302 (2016).
110. Huang, W. *et al.* circRNA circAF4 functions as an oncogene to regulate MLL-AF4 fusion protein expression and inhibit

MLL leukemia progression. *J. Hematol. Oncol.* **12**, 103 (2019).
111. Shang, J. *et al.* CircPAN3 mediates drug resistance in acute myeloid leukemia through the miR-153-5p/miR-183-5p–XIAP axis. *Exp. Hematol.* **70**, (2019).
112. Costa-Mattioli, M. & Walter, P. The integrated stress response: From mechanism to disease. *Science* **368**, (2020).
113. Pakos-Zebrucka, K. *et al.* The integrated stress response. *EMBO Rep.* **17**, 1374–1395 (2016).
114. Tameire, F. *et al.* ATF4 couples MYC-dependent translational activity to bioenergetic demands during tumour progression. *Nat. Cell Biol. 2019 217* **21**, 889–899 (2019).
115. Lu, P. D., Harding, H. P. & Ron, D. Translation reinitiation at alternative open reading frames regulates gene expression in an integrated stress response. *J. Cell Biol.* **167**, 27–33 (2004).
116. Wortel, I. M. N., van der Meer, L. T., Kilberg, M. S. & van Leeuwen, F. N. Surviving Stress: Modulation of ATF4-Mediated Stress Responses in Normal and Malignant Cells. *Trends Endocrinol. Metab.* **28**, 794 (2017).
117. Gardner, B. M., Pincus, D., Gotthardt, K., Gallagher, C. M. & Walter, P. Endoplasmic Reticulum Stress Sensing in the Unfolded Protein Response. *Cold Spring Harb. Perspect. Biol.* **5**, (2013).
118. Chen, M. & Xie, S. Therapeutic targeting of cellular stress responses in cancer. *Thorac. Cancer* **9**, 1575 (2018).
119. Moloney, J. N. & Cotter, T. G. ROS signalling in the biology of cancer. *Semin. Cell Dev. Biol.* **80**, 50–64 (2018).
120. Wei, J. *et al.* HRD1-mediated METTL14 degradation regulates m6A mRNA modification to suppress ER proteotoxic liver disease. *Mol. Cell* **81**, 5052-5065.e6 (2021).
121. Li, Q. *et al.* NSUN2-mediated m5C methylation and METTL3/METTL14-mediated m6A methylation cooperatively enhance p21 translation. *J. Cell. Biochem.*

118, 2587 (2017).
122. Zhao, T., Li, X., Sun, D. & Zhang, Z. Oxidative stress: One potential factor for arsenite-induced increase of N6-methyladenosine in human keratinocytes. *Environ. Toxicol. Pharmacol.* **69**, 95–103 (2019).
123. Sun, L. *et al.* RNA-binding protein RALY reprogrammes mitochondrial metabolism via mediating miRNA processing in colorectal cancer. *Gut* **70**, 1698–1712 (2021).
124. Wang, J. *et al.* METTL3/m6A/miRNA-873-5p attenuated oxidative stress and apoptosis in colistin-induced kidney injury by modulating Keap1/Nrf2 pathway. *Front. Pharmacol.* **10**, (2019).
125. Zhang, Y. *et al.* The Role of miRNAs during Endoplasmic Reticulum Stress Induced Apoptosis in Digestive Cancer. *J. Cancer* **12**, 6787 (2021).
126. Zhao, T., Du, J. & Zeng, H. Interplay between endoplasmic reticulum stress and non-coding RNAs in cancer. *J. Hematol. Oncol.* **13**, 163 (2020).
127. Du, W. W. *et al.* Foxo3 circular RNA promotes cardiac senescence by modulating multiple factors associated with stress and senescence responses. *Eur. Heart J.* **38**, 1402–1412 (2017).
128. Eskelinen, E. L. Autophagy: Supporting cellular and organismal homeostasis by self-eating. *Int. J. Biochem. Cell Biol.* **111**, 1–10 (2019).
129. Yun, C. W. & Lee, S. H. The Roles of Autophagy in Cancer. *Int. J. Mol. Sci.* **19**, (2018).
130. Chen, X. *et al.* METTL3-mediated m6A modification of ATG7 regulates autophagy-GATA4 axis to promote cellular senescence and osteoarthritis progression. *Ann. Rheum. Dis.* **81**, 87–99 (2022).
131. Li, Q. *et al.* HIF-1α-induced expression of m6A reader YTHDF1 drives hypoxia-induced autophagy and malignancy of hepatocellular carcinoma by promoting ATG2A and ATG14 translation. *Signal Transduct. Target.*

Ther. **6**, (2021).
132. Liang, G. *et al.* Autophagy-associated circRNA circCDYL augments autophagy and promotes breast cancer progression. *Mol. Cancer* **19**, 1–16 (2020).
133. Hetz, C., Axten, J. M. & Patterson, J. B. Pharmacological targeting of the unfolded protein response for disease intervention. *Nat. Chem. Biol.* **15**, 764–775 (2019).
134. Śniegocka, M., Liccardo, F., Fazi, F. & Masciarelli, S. Understanding ER homeostasis and the UPR to enhance treatment efficacy of acute myeloid leukemia. *Drug Resist. Updat.* **64**, (2022).
135. Scott, K., Hayden, P. J., Will, A., Wheatley, K. & Coyne, I. Bortezomib for the treatment of multiple myeloma. *Cochrane Database of Systematic Reviews* (2016). doi:10.1002/14651858.CD010816.pub2
136. Wu, J. *et al.* N6-Methyladenosine Modification Opens a New Chapter in Circular RNA Biology. *Front. Cell Dev. Biol.* **9**, (2021).
137. Way, S. W. & Popko, B. Harnessing the integrated stress response for the treatment of multiple sclerosis. *Lancet. Neurol.* **15**, 434–443 (2016).
138. Liu, M., Wang, Q., Shen, J., Yang, B. B. & Ding, X. Circbank: a comprehensive database for circRNA with standard nomenclature. *RNA Biol.* **16**, 899–905 (2019).
139. Shallis, R. M., Wang, R., Davidoff, A., Ma, X. & Zeidan, A. M. Epidemiology of acute myeloid leukemia: Recent progress and enduring challenges. *Blood Rev.* **36**, 70–87 (2019).
140. Loke, J., Buka, R. & Craddock, C. Allogeneic Stem Cell Transplantation for Acute Myeloid Leukemia: Who, When, and How? *Front. Immunol.* **12**, 1182 (2021).
141. Féral, K. *et al.* ER Stress and Unfolded Protein Response in Leukemia: Friend, Foe, or Both? *Biomolecules* **11**, 1–31 (2021).
142. Hetz, C. & Chevet, E. Theme Series – UPR in cancer.

Semin. Cancer Biol. **33**, 1–2 (2015).
143. Doultsinos, D. *et al.* Control of the Unfolded Protein Response in Health and Disease. *SLAS Discov. Adv. life Sci. R D* **22**, 787–800 (2017).
144. Masciarelli, S. *et al.* Retinoic acid and arsenic trioxide sensitize acute promyelocytic leukemia cells to ER stress. *Leukemia* (2018). doi:10.1038/leu.2017.231
145. Masciarelli, S. *et al.* Retinoic acid synergizes with the unfolded protein response and oxidative stress to induce cell death in FLT3-ITD+ AML. *Blood Adv.* **3**, 4155–4160 (2019).
146. Liu, J., Zhao, R., Jiang, X., Li, Z. & Zhang, B. Progress on the Application of Bortezomib and Bortezomib-Based Nanoformulations. *Biomolecules* **12**, (2021).
147. Huang, J. & Yin, P. Structural Insights into N6-methyladenosine (m6A) Modification in the Transcriptome. *Genomics. Proteomics Bioinformatics* **16**, 85–98 (2018).
148. Sang, L. *et al.* The m6A RNA methyltransferase METTL3/METTL14 promotes leukemogenesis through the mdm2/p53 pathway in acute myeloid leukemia. *J. Cancer* **13**, 1019 (2022).
149. Greene, J. *et al.* Circular RNAs: Biogenesis, Function and Role in Human Diseases. *Front. Mol. Biosci.* **4**, 38 (2017).
150. Zhang, L. *et al.* Bone Marrow Mesenchymal Stem Cells-Derived Exosomal miR-425-5p Inhibits Acute Myeloid Leukemia Cell Proliferation, Apoptosis, Invasion and Migration by Targeting WTAP. *Onco. Targets. Ther.* **14**, 4901–4914 (2021).
151. Wek, R. C., Jiang, H.-Y. & Anthony, T. G. Coping with stress: eIF2 kinases and translational control. *Biochem. Soc. Trans.* **34**, 7 (2006).
152. Teske, B. F., Baird, T. D. & Wek, R. C. Methods for Analyzing eIF2 Kinases and Translational Control in the Unfolded Protein Response. *Methods Enzymol.* **490**, 333–356 (2011).

153. Powers, E. N. & Brar, G. A. m6A and eIF2α-Ⓟ Team Up to Tackle ATF4 Translation during Stress. *Mol. Cell* **69**, 537–538 (2018).
154. Pedre, B., Barayeu, U., Ezeriņa, D. & Dick, T. P. The mechanism of action of N-acetylcysteine (NAC): The emerging role of H2S and sulfane sulfur species. *Pharmacol. Ther.* **228**, 107916 (2021).
155. Liu, X. *et al.* CircRNF220, not its linear cognate gene RNF220, regulates cell growth and is associated with relapse in pediatric acute myeloid leukemia. *Mol. Cancer* **20**, 1–18 (2021).
156. Ge, R. & Gao, G. Anti-antioxidant impacts of circZNF609 silence in HaCaT cells through regulating miR-145. *https://doi.org/10.1080/21691401.2019.1709863* **48**, 384–392 (2020).
157. Wang, J. J. *et al.* Circular RNA-ZNF609 regulates retinal neurodegeneration by acting as miR-615 sponge. *Theranostics* **8**, 3408 (2018).
158. Zhou, J. *et al.* CircHIPK3: Key Player in Pathophysiology and Potential Diagnostic and Therapeutic Tool. *Front. Med.* **8**, 170 (2021).
159. Wang, Y. *et al.* Exosomal circHIPK3 Released from Hypoxia-Pretreated Cardiomyocytes Regulates Oxidative Damage in Cardiac Microvascular Endothelial Cells via the miR-29a/IGF-1 Pathway. *Oxid. Med. Cell. Longev.* **2019**, (2019).
160. Richard-Carpentier, G. & DiNardo, C. D. Venetoclax for the treatment of newly diagnosed acute myeloidleukemia in patients who are ineligible for intensivechemotherapy. *Ther. Adv. Hematol.* **10**, 204062071988282 (2019).
161. Lam, S. S. Y. & Leung, A. Y. H. Overcoming Resistance to FLT3 Inhibitors in the Treatment of FLT3-Mutated AML. *Int. J. Mol. Sci.* **21**, (2020).
162. Konopleva, M. Y. Mechanisms for resistance in AML insights into molecular pathways mediating resistance to

venetoclax. *Best Pract. Res. Clin. Haematol.* **34**, (2021).
163. Ewels, P., Magnusson, M., Lundin, S. & Käller, M. MultiQC: summarize analysis results for multiple tools and samples in a single report. *Bioinformatics* **32**, 3047–3048 (2016).
164. Dobin, A. *et al.* STAR: ultrafast universal RNA-seq aligner. *Bioinformatics* **29**, 15–21 (2013).
165. Ma, X. K., Xue, W., Chen, L. L. & Yang, L. CIRCexplorer pipelines for circRNA annotation and quantification from non-polyadenylated RNA-seq datasets. *Methods* **196**, 3–10 (2021).
166. Zhang, J., Chen, S., Yang, J. & Zhao, F. Accurate quantification of circular RNAs identifies extensive circular isoform switching events. *Nat. Commun. 2020 111* **11**, 1–14 (2020).

LIST OF PUBLICATIONS

- Liccardo F, Iaiza A, Śniegocka M, et al. Circular RNAs Activity in the Leukemic Bone Marrow Microenvironment. Noncoding RNA. 2022 Jul 1;8(4):50. doi: 10.3390/ncrna8040050. PMID: 35893233; PMCID: PMC9326527.

- Turco C, Esposito G, Iaiza A, et al. MALAT1-dependent hsa_circ_0076611 regulates translation rate in triple-negative breast cancer. Commun Biol. 2022 Jun 16;5(1):598. doi: 10.1038/s42003-022-03539-x. PMID: 35710947; PMCID: PMC9203778.

- Iaiza A, Tito C, Ganci F, et al. Long Non-Coding RNAs in the Cell Fate Determination of Neoplastic Thymic Epithelial Cells. Front Immunol. 2022 Apr 22;13:867181. doi: 10.3389/fimmu. 2022.867181. PMID: 35529877; PMCID: PMC9073009.

- Iaiza A, Tito C, Ianniello Z, et al. METTL3-dependent MALAT1 delocalization drives c-Myc induction in thymic epithelial tumors. Clin Epigenetics. 2021 Sep 16;13(1):173. doi: 10.1186/s13148-021-01159-6. PMID: 34530916; PMCID: PMC8447796.

- Ianniello Z, Sorci M, Ceci Ginistrelli L, et al. New insight into the catalytic -dependent and -independent roles of METTL3 in sustaining aberrant translation in chronic myeloid leukemia. Cell Death Dis. 2021 Sep 24;12(10):870. doi: 10.1038/s41419-021-04169-7. PMID: 34561421.

- Tito C, De Falco E, Rosa P, et al. Circulating microRNAs from the Molecular Mechanisms to Clinical Biomarkers: A

Focus on the Clear Cell Renal Cell Carcinoma. Genes (Basel). 2021 Jul 28;12(8):1154. doi: 10.3390/genes12081154. PMID: 34440329; PMCID: PMC8391131.

- Tito C, Ganci F, Sacconi A, et al. LINC00174 is a novel prognostic factor in thymic epithelial tumors involved in cell migration and lipid metabolism. Cell Death Dis. 2020 Nov 7;11(11):959. doi: 10.1038/s41419-020-03171-9. PMID: 33161413; PMCID: PMC7648846.

- Petrozza V, Costantini M, Tito C, et al. Emerging role of secreted miR-210-3p as potential biomarker for clear cell Renal Cell Carcinoma metastasis. Cancer Biomark. 2020;27(2):181-188. doi: 10.3233/CBM-190242. PMID: 31771042.

POINT BY POINT RESPONSE TO THE REVIEWERS

1st Reviewer: Colotti Gianni
Accept as is

The thesis "Role of m^{6}A-dependent circRNAs during stress response in myeloid leukemic cells", by Alessia Iaiza, deals with an important biological issue, i.e. the relationship between the factors of the important m^{6}A RNA modification and the suppression of the proteotoxic stress response, whose induction is emerging as a relevant anticancer therapy in Acute Myeloid Leukemia (AML). The thesis investigates the effect of Bortezomib, a proteasome inhibitor, on the expression of the enzymes involved in m6A formation: the work shows that that treatment of AML cells with Bortezomib induces m^{6}A enzymes downregulation at translation level, due to ROS generation and activation of the oxidative stress response; further, the thesis investigates the impact of bortezomib on the modulation of m^{6}A-dependent circRNAs expression, showing that their expression and methylation is increased by the drug. The thesis opens the field toward a possible use of m^{6}A-dependent circRNAs as molecular targets to improve bortezomib efficacy in AML. The thesis is well thought and well written. The data shown are relevant for the field of research on AML, and their presentation is clear and coherent.

I really thank the reviewer for the positive comments and for appreciating my PhD's thesis

2nd Reviewer: Di Agostino Silvia
Minor revision

This thesis is titled "Role of m^{6}A-dependent circRNAs during stress response in myeloid leukemic cells" by PhD student Alessia Iaiza. First of all, this is an excellent doctoral thesis with a very high

novelty of the topic and it must be evaluated on different levels. First, from the point of view of the content, Dr. Iaiza has been entrusted with an ambitious project that involves the dissection of a molecular mechanism that constitutes a pathway, in a difficult and articulated tumor model such as that of AML, where uncovered crosstalk recently emerged between AML cells and bone marrow niche. This finding is driving the field to numerous studies to search for new therapeutic targets. Second, the rationale of the thesis is very robust and convincing, the structure of the "Introduction" is precise, and the various steps of the mechanism and the role of the different molecules are described by a very fluent way. In general, the whole thesis is well written. Third, the design of the experiments well supports the aims expressed by the candidate (Section 3). The quality of the experimental part is very good.

I thank the reviewer for the interest in my PhD's project and for the suggestions proposed.

Minor observations:

- Figure 4.1 and 4.7: I would like to suggest inserting, together with the quantization in percentage of positive PI dead cells, some representative images of the populations from cytofluorimetric analysis with the various treatments.

I thank the reviewer for this suggestion. I have added in the thesis representative images of the populations from cytofluorimetric analysis, both in Figure 4.1B and in Figure 4.7B.

- In view of a publication of these data, the candidate should seek to generate a second cell line resistant to Btz. This would undoubtedly make the finding even more robust

The reviewer is right, it could be very important to generate a different cell line resistant to Btz. For sure, we could use another

AML cell line, MV4-11 cell line, in order to perform the same experiments that we have performed in MOLM13 cells (m^6A enzyme mRNA and protein expression levels, ISR induction and ROS levels analysis) and, once we assessed that Btz has the same effects also in this cell line, we could generate MV4-11 cell line resistant to Btz.

- Since the thesis makes use of many analysis techniques, it would be useful in the introduction or in the AIMS to insert a flowchart that schematically illustrates the experimental design followed

I thank the reviewer for this comment, and I have now provided a flowchart of experimental design followed, at the end of the section entitled "Aims".

- In the section of the "Discussion", it would be useful to insert a final figure of the disserted mechanism

I thank the reviewer for this useful suggestion. I have now inserted a final figure as Figure 5.1, in the section "Conclusion", that represent the disserted mechanism proposed in my thesis.